AD-A122 871 A PHOTOELECTRON MODEL FOR THE RAPID COMPUTATION OF ATMOSPHERIC EXCITATION RATES(U) NAVAL RESEARCH LAB WASHINGTON DC D J STRICKLAND ET AL. 30 DEC 82 1/1

UNCLASSIFIED NRL-MR-5004 F/G 7/4 NL

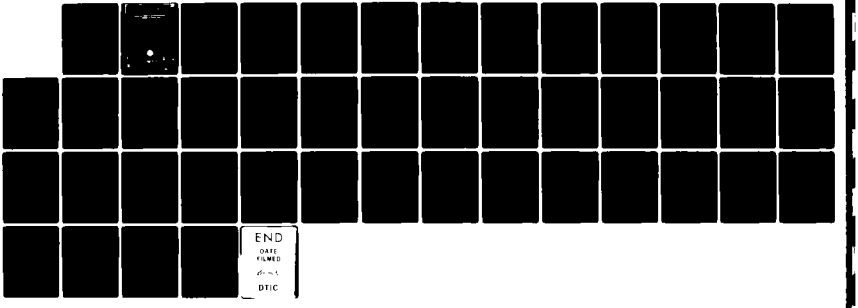

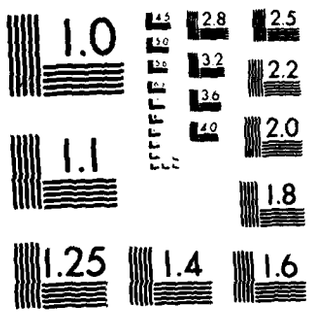

SECURITY CLASSIFICATION OF THIS PAGE (When Data Entered)

REPORT DOCUMENTATION PAGE	READ INSTRUCTIONS BEFORE COMPLETING FORM
1. REPORT NUMBER: NRL Memorandum Report 5004	2. GOVT ACCESSION NO.: A122 841
3. RECIPIENT'S CATALOG NUMBER:	
4. TITLE (and Subtitle): A PHOTOELECTRON MODEL FOR THE RAPID COMPUTATION OF ATMOSPHERIC EXCITATION RATES	5. TYPE OF REPORT & PERIOD COVERED: Interim report on a continuing NRL problem.
	6. PERFORMING ORG. REPORT NUMBER:
7. AUTHOR(s): D.J. Strickland* and R.R. Meier	8. CONTRACT OR GRANT NUMBER(s):
9. PERFORMING ORGANIZATION NAME AND ADDRESS: Naval Research Laboratory, Washington, DC 20375	10. PROGRAM ELEMENT, PROJECT, TASK AREA & WORK UNIT NUMBERS: 61153N; RR034-06-42; 41-0939-0-3
11. CONTROLLING OFFICE NAME AND ADDRESS:	12. REPORT DATE: December 30, 1982
	13. NUMBER OF PAGES: 43
14. MONITORING AGENCY NAME & ADDRESS(if different from Controlling Office):	15. SECURITY CLASS. (of this report): UNCLASSIFIED
	15a. DECLASSIFICATION/DOWNGRADING SCHEDULE:

16. DISTRIBUTION STATEMENT (of this Report)

Approved for public release; distribution unlimited.

17. DISTRIBUTION STATEMENT (of the abstract entered in Block 20, if different from Report)

18. SUPPLEMENTARY NOTES

*Present address: Beers Associates, Incorporated, P.O. Box 2547, Reston, VA 22090

19. KEY WORDS (Continue on reverse side if necessary and identify by block number)

Photoelectrons
Dayglow
Photoionization
Atmospheric excitation rates

20. ABSTRACT (Continue on reverse side if necessary and identify by block number)

This report describes a model for excitation and ionization in the daytime ionosphere. The model was developed to study optical emissions under a variety of conditions. The needed photoelectron flux is calculated using an integral equation which provides for a detailed energy loss description but does not include transport effects. Currently, the calculated flux is used to specify altitude profiles of volume excitation rates for approximately 50 processes. A brief description is given of the computational model along with

(Continues)

DD FORM 1 JAN 73 1473 EDITION OF 1 NOV 65 IS OBSOLETE
S/N 0102-014-6601

SECURITY CLASSIFICATION OF THIS PAGE (When Data Entered)

20. ABSTRACT (Continued)

tests and comparisons which were made for validation purposes. A listing is provided which gives the energy dependences of all applied electron impact cross sections. This is accompanied by tables which give the corresponding references. Results include calculated photoelectron flux spectra and altitude profiles of volume production rates for a variety of processes under various atmospheric and solar conditions.

CONTENTS

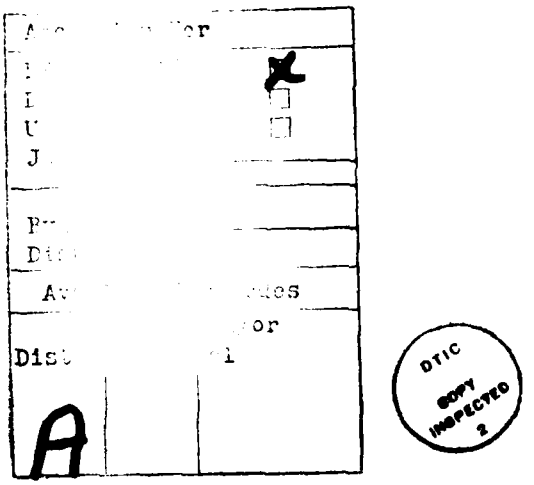

A PHOTOELECTRON MODEL FOR THE RAPID COMPUTATION OF ATMOSPHERIC EXCITATION RATES

I. INTRODUCTION

Recently, experiments flown on rockets and satellites have delivered high quality far and extreme ultraviolet spectra of the ionospheric dayglow (Gentieu et al., 1979; Meier et al., 1980; Anderson et al., 1980a, b; Huffman et al., 1980; Feldman et al., 1981; Gentieu et al., 1981). Since many of the spectral features between 500 and 2000 Å are produced by photoelectron impact excitation, dissociation, and ionization, there is a need for a model which can rapidly provide the steady state photoelectron energy spectrum to be used for the computation of excitation rates. While a number of photoelectron models are already in existence, they are not typically suited to computation of excitation rates under a variety of atmospheric and solar conditions because of long computer times.

The model we have developed ignores photoelectron transport (a valid approximation up to at least 300 km). The code allows selection of any one of the five solar spectra given by Torr et al. (1979), an atmospheric model from Jacchia (1971 or 1977), and the solar zenith angle. The output is the photoelectron flux vs. energy and excitation rates for 26 states of N_2, 13 states of O_2, and 7 states of O, including selected other rates for N, N^+, and O^+, all as functions of altitude from 100 - 450 km. The total computation time for a complete altitude profile on the NRL Texas Instrument ASC is about 7 sec.

II. DESCRIPTION OF THE PHOTOELECTRON CODE

The photoelectron code solves for the steady-state photoelectron flux and associated excitation and ionization rates in the local approximation; that is, transport is ignored. Insignificant error in altitude profiles of emission rates occurs as a result of this approximation. This is due to the softness of the photoelectron spectrum, which leads to mostly local energy deposition of electrons.

The code (commonly referred to as PEGFAC as an acronym for photo-electron g-factors) is actually a set of three codes. Figure 1 shows their functions in terms of input and output information. We label the codes by the following names:

1) SOURCE
2) MATRIX
3) FLUX

Manuscript approved November 17, 1982.

The calculation begins with code SOURCE. The code sets up a model atmosphere (Jacchia, 1971 or 1977) which is used to attenuate the selected solar flux and specify the photoelectron source spectrum. The source spectrum is obtained from several hundred km down to about 100 km. At each point on the chosen altitude grid, integrations over energy, $h\nu$, are performed. Each integrand is the product of the attenuated solar spectrum, a partial photoionization cross section, and density of the ionizing species. The numbers of ion states considered for N_2, O_2, and O are 5, 10, and 5, respectively.

For a given run, SOURCE uses one of five available solar spectra. These come from Torr et al. (1979) and are used to represent the spectrum under various solar activity conditions. At short wavelengths (below 200 Å), their band averaged flux values have been replaced by a set of fluxes for lines spanning the wavelength range 7.5 Å to 190 Å (Donnelly and Pope, 1973). A scaling factor allows for an overall magnitude change in this set of values from run to run.

The outputs from code SOURCE are S(z,E), the photoelectron source spectrum, the model atmosphere ($n(N_2)$, $n(O_2)$, n(O), and T vs. altitude z), and the energy grid needed to specify S as well as flux ϕ.

Code MATRIX provides the energy loss matrix needed to solve for the photoelectron flux. The starting integral equation is

$$0 = -\sum_{\ell} n_{\ell}(z)\,\sigma_{\ell}(E)\phi(z,E) + \sum_{\ell} n_{\ell}(z) \sum_{k} \int_{E}^{E_{max}} \sigma_{\ell k}(E',E)\phi(z,E')dE' + n_p \frac{\partial}{\partial E}\left[L_p(E)\phi(z,E)\right] + S(z,E) \qquad (1)$$

with terms defined as follows:

ϕ	photoelectron flux in electrons $cm^{-2}s^{-1}eV^{-1}$
S	source spectrum in electrons $cm^{-3}s^{-1}eV^{-1}$
n_{ℓ}	density of ℓ^{th} neutral species (N_2, O_2, and O treated)
σ_{ℓ}	total inelastic cross section of ℓ^{th} species involved
$\sigma_{\ell k}$	inelastic cross section for the k^{th} process of the ℓ^{th} species in cm^2/eV
n_p	plasma density
L_p	loss function for energy loss to the plasma.

Equation (1) is replaced by a matrix equation expressed in the form

$$0 = \sum_{\ell} n_{\ell} \sum_{j \le i} R_{ij}^{\ell} \phi_j(z) + n_p \frac{\partial}{\partial E} \left[L_p(E) \phi(z,E) \right]_{E_i} + S_i(z) \qquad (2)$$

The matrix R is generated in code MATRIX for each species. The technique for approximating the integral in equation (1) is the same used by Strickland et al. (1976) for the energy dependence of their more general equation.

Code FLUX solves equation (2) for flux $\phi(z,E)$ and subsequently obtains associated excitation rates and g-factors. The excitation rate, designated by $P_{\ell k}(z)$ is

$$P_{\ell k}(z) = n_{\ell}(z) \int_{W_{\ell k}}^{E_{max}} \sigma_{\ell k}(E) \phi(z,E) dE \qquad (3)$$

where $W_{\ell k}$ is an excitation threshold and index k refers to either an excitation or ionization process. Three sets of rates are determined for impact on N_2, O_2, and O. The g-factor, or rate of excitation ($atom^{-1}s^{-1}$), designated by $g_{\ell k}(z)$ is

$$g_{\ell k}(z) = \int_{W_{\ell k}}^{E_{max}} \sigma_{\ell k}(E) \phi(z,E) dE \qquad (4)$$

Four sets of g-factors are determined, with the first three corresponding to the sets of production rates. The fourth set allows for excitations not involving impact on N_2, O_2, and O. Several processes are presently included in this set involving impact excitation of NI and OII.

III. CODE VALIDATION

In this section, we discuss the validation of the code and applied data set. This has been done by applying an energy conservation test and comparing the photoelectron flux with other calculated values and with measured results. The applied test determines how well the following equality holds:

$$\sum_{\ell,k} W_{\ell k} P_{\ell k} + n_p \int_{E_{min}}^{E_{max}} L_p(E) \phi(z,E) dE = \int_{E_{min}}^{E_{max}} S(z,E) E dE \qquad (5)$$

The conservation principle states that the rate of energy transfer to the ion and excited states and to the plasma equals the rate of energy going into the photoelectron source spectrum. We find that equation (5) is satisfied in our calculations to better than 15% over the altitude range of interest.

The energy conservation test is useful for determining the accuracy of the representation of equation (1) by equation (2) and accuracy of the numerical procedures within the code. Once it is established that the computational model is working, comparisons of the results with independent values are useful for testing the input data which include the model atmosphere, photon and electron impact cross sections, and the solar spectrum. We have compared our photoelectron flux spectrum with data by Lee et al., (1980), a calculated spectrum provided by E. Oran (see Oran and Strickland, 1978), and a photoelectron spectrum computed by Knut Stamnes (1982, private communication).

The Lee et al. data we compare with were obtained under quiet solar conditions at a solar zenith angle of 10° and an altitude of 190 km. Figure 2 shows our first comparison over an energy range from a few eV to 75 eV. For the calculations, the Torr et al. solar spectrum labeled with an $F_{10.7}$ value of 71 was used which corresponds to low solar activity. If we use one of the higher activity spectra the agreement is not as good. This is seen in Figure 3 where the spectrum labeled with an $F_{10.7}$ value of 206 has been used. Based on these comparisons, the applied low activity spectrum appears to adequately represent conditions at the time of the observation.

The results calculated by Oran were obtained for moderate solar activity at a solar zenith angle of 56°. Figure 4 shows the comparisons at altitudes of 210 and 150 km. Oran's results include the effect of transport and are based on the solar spectrum reported by Donnelly and Pope (1973). We have used the high activity solar spectrum cited above which corresponds to $F_{10.7} = 206$.

The comparison with the photoelectron calculation of Knut Stamnes corresponds to an overhead sun, solar 10.7 cm flux of 68, and an exospheric temperature of 1000 K. Again, the agreement is quite good. However, it is not shown because the atmospheric model used by Stamnes was considerably different than that used in the present examples.

To summarize, our initial code validation effort suggests we may now proceed to meaningful photoelectron excited dayglow studies. This is based on good energy conservation and the flux comparisons just described.

IV. INPUT/OUTPUT DESCRIPTION

The calculation of photoelectron spectra and associated volume excitation rates requires a large body of input data. These data were previously identified in Figure 1. In this section, we will discuss the extent of the needed parameters.

A large body of output information is also generated in the form of source spectra, flux spectra, excitation rates, and g-factors. A discussion is included of these quantities, in particular, of the types of excitation processes which have been considered.

The input information may be catagorized as follows:

- model atmosphere
- solar spectrum (EUV to X-ray)
- photoabsorption cross sections
- partial photoionization cross sections
- inelastic cross sections for modeling the photoelectron energy degradation
- loss function for energy loss to plasma

and

- excitation cross sections for specifying excitation processes of interest.

Some of these quantities have already been discussed. Nevertheless, we will briefly address each of them here, noting either their source or extent. The model atmosphere comes from Jacchia (1971 or 1977) and is generated in code SOURCE once the exospheric temperature, T_∞, is specified. We allow for a scaling of the O density through a factor appearing in the input data.

The solar flux values come from Torr et al. (1979) and Donnelly and Pope (1973). In a given run, one of the five available spectra in the input data set to SOURCE is selected depending on the degree of solar activity to be modeled. A combination of line and continuum band fluxes totaling 38 in number is provided with the Torr et al. spectra. We have replaced their short wavelength band fluxes (<200 Å) with line fluxes from Donnelly and Pope (1973). A scaling factor has been introduced to

allow experimentation on our part for lack of knowledge of how the soft X-ray flux varies with time. Figures 5 and 6 show plots of the input solar spectra for low and high solar activity.

The total absorption cross sections are used to specify the attenuated solar spectrum. They come from Torr et al. (1979). The partial ionization cross sections come from Kirby et al. (1979) and selected papers referenced therein. Photoionization is modeled for five states of N_2^+, ten states of O_2^+, and five states of O^+. The ionization thresholds span an energy range from 12.1 to 25 eV.

There are two sets of electron impact cross sections. The first set defines the energy loss matrix elements while the second set allows for excitation to states of specific interest to dayglow studies. In terms of energy loss, the latter is a subset of the former. Most of the applied cross sections come from the previous work of Strickland. These may be found in the papers by Strickland et al. (1976) and Oran and Strickland (1978). Recently, members have been added for processes such as dissociative ionization of N_2 leading to NII 1085 Å. Most of these have come from measurements by E.C. Zipf and colleagues. A tabular listing of the cross sections and references is given in the appendix.

The final parameter on the above list is the loss function for energy loss to the plasma. It should be noted that such loss is not important to the study of the UV dayglow. Electron impact excitation leading to UV emission is primarily at electron energies above 10 eV while plasma absorption of the photoelectron energy affecting the flux spectrum occurs below this energy. In spite of this, we include the effects of plasma energy loss so as not to exclude the low energy region from future studies. The applied loss function comes from Schunk and Hays (1971).

We will now briefly describe the output information. The flux $\phi(z,E)$ is currently calculated for ~40 altitudes between 400 and 100 km and for as many as 75 energies. Approximately 40 excitation rates and 48 g-factors are specified on the altitude grid. These refer to ionization, vibrational excitation, electronic state excitation of the states producing important energy loss, and additional processes leading to UV emission at selected wavelengths. The excited state species producing the emission's include N_2, N_2^+, O, O^+, N, and N^+. Some of the features will be addressed in the next section.

V. RESULTS

In this section, volume excitation rates will be presented, most of which lead to familiar UV dayglow features. Our intent here is to illustrate the nature of some of the results being generated rather than to address a specific problem in the study of the UV dayglow.

Two sets of results will be presented. Set 1 appears in Figure 7-12 and applies to the same model atmosphere, solar spectrum, and solar zenith angle (SZA). Set 2 appears in Figures 13-18 and shows how the $O(^5S)$ and $N_2(a^1\Pi_g)$ rates change with variations in the above parameters. For set 1, the following conditions apply: $F_{10.7} = 206$, $T_\infty = 1000°$ K, SZA = 56°, and n(O) is ½ of the value from Jacchia (1971). (FRACO = ½.)

Beginning with set 1, the total ionization rates for N_2, O_2 and O are shown in Figure 7. The rates for N_2 and O_2 contain contributions from dissociative ionization. Two important excited states of N_2 are the $C^3\Pi$ and $a^1\Pi_g$ states since they lead to the second positive and LBH Band systems. Figure 8 shows the excitation rates for these states. In Figure 9, we compare the $a^1\Pi_g$ rate with another important one, namely that for the $OI(^5S)$ state. The ^5S and ^3S rates are seen together in Figure 10. Strong photon imprisonment of 1304 Å photons will greatly amplify the ^3S production rate shown in this figure.

The last results of the first set are for dissociative excitation. It should be kept in mind that for some of the features to be shown, direct excitation of the atomic species will dominate the dissociative process. This is especially true for the OI emissions, due to the large amount of atomic oxygen relative to O_2 present in the important excitation region. Figure 11 shows dissociative excitation rates for producing emission in the features NI 1200 Å, NI 1134 Å, NI 1493 Å, and NI 1243 Å. Figure 12 shows rates for producing emission at OI 1304 Å, OI 1356 Å, OI 1027 Å, and OI 989 Å.

For set 2, the results apply to the three cases identified in Table 1. For each case, several solar zenith angles are considered as given in the table. Figures 13-15 show the production rates for $O(^5S)$ with each figure referring to a different case. Similar results for $N_2(a^1\Pi_g)$ appear in Figures 16-18. Noteworthy features of the results in set 2 are an approximate doubling of the rates in going from low to high solar activity and the respective decreases and increases in the ^5S and $a^1\Pi_g$ rates as n(O) is

scaled from .5 to .25 times the Jacchia (1971) value. The ^5S rates vary almost directly with n(0) as expected.

Table 1. Cases for which results have been obtained with the photoelectron code. For each case, the following solar zenith angles were treated: 0°, 30°, 60°, 75°, 83°, 87°, and 90°.

Case	n(0) Scaling Factor	T(°K)	$F_{10.7}$
1	.5	1000	71
2	.5	1000	206
3	.25	1000	206

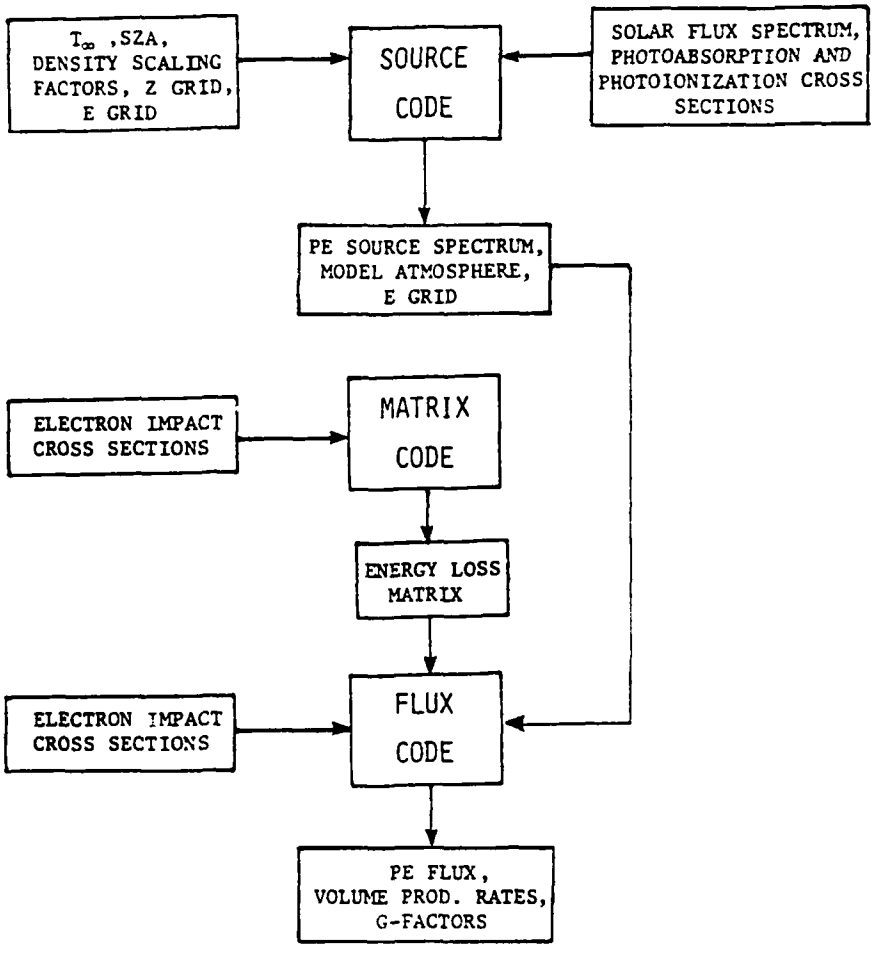

Fig. 1. Block diagram for the applied photoelectron code.

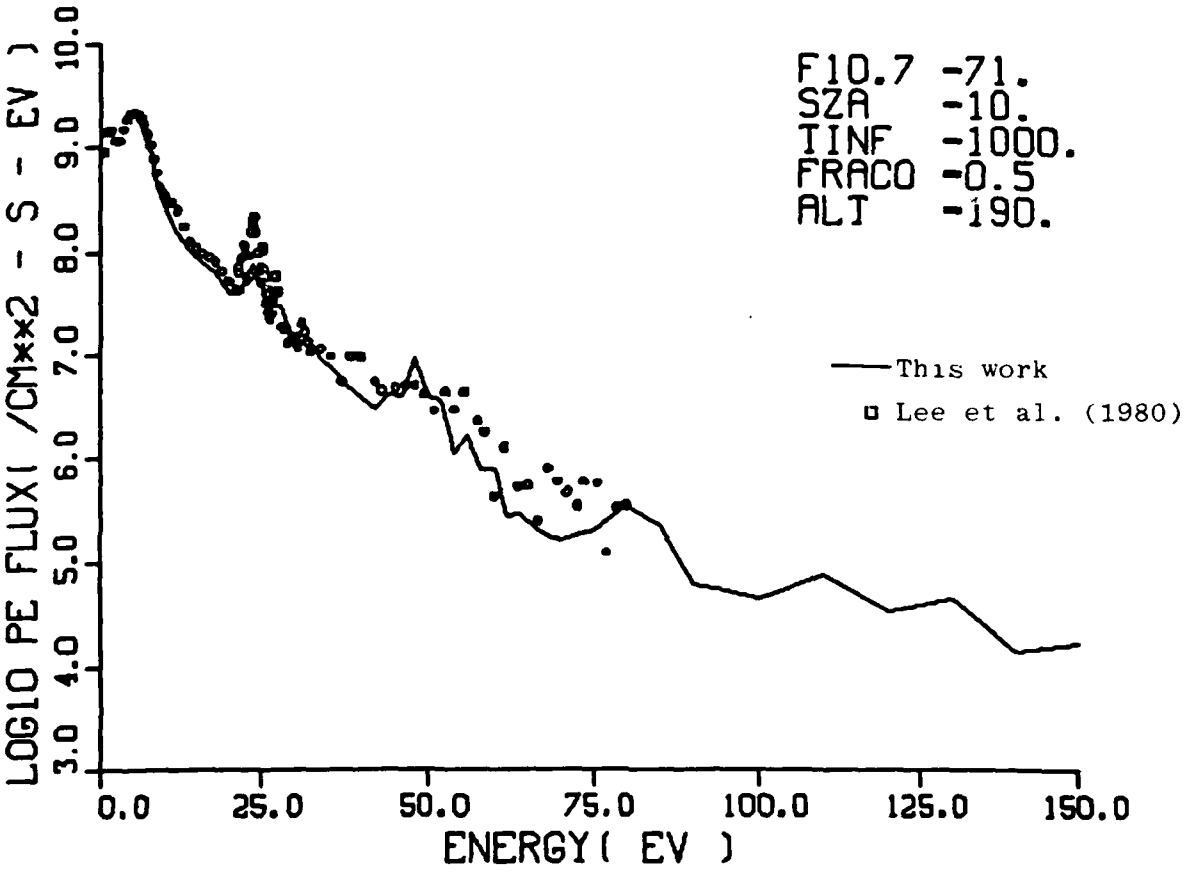

Fig. 2. 4π integrated photoelectron flux. Both profiles correspond to low solar activity. FRACO is the O density scaling factor.

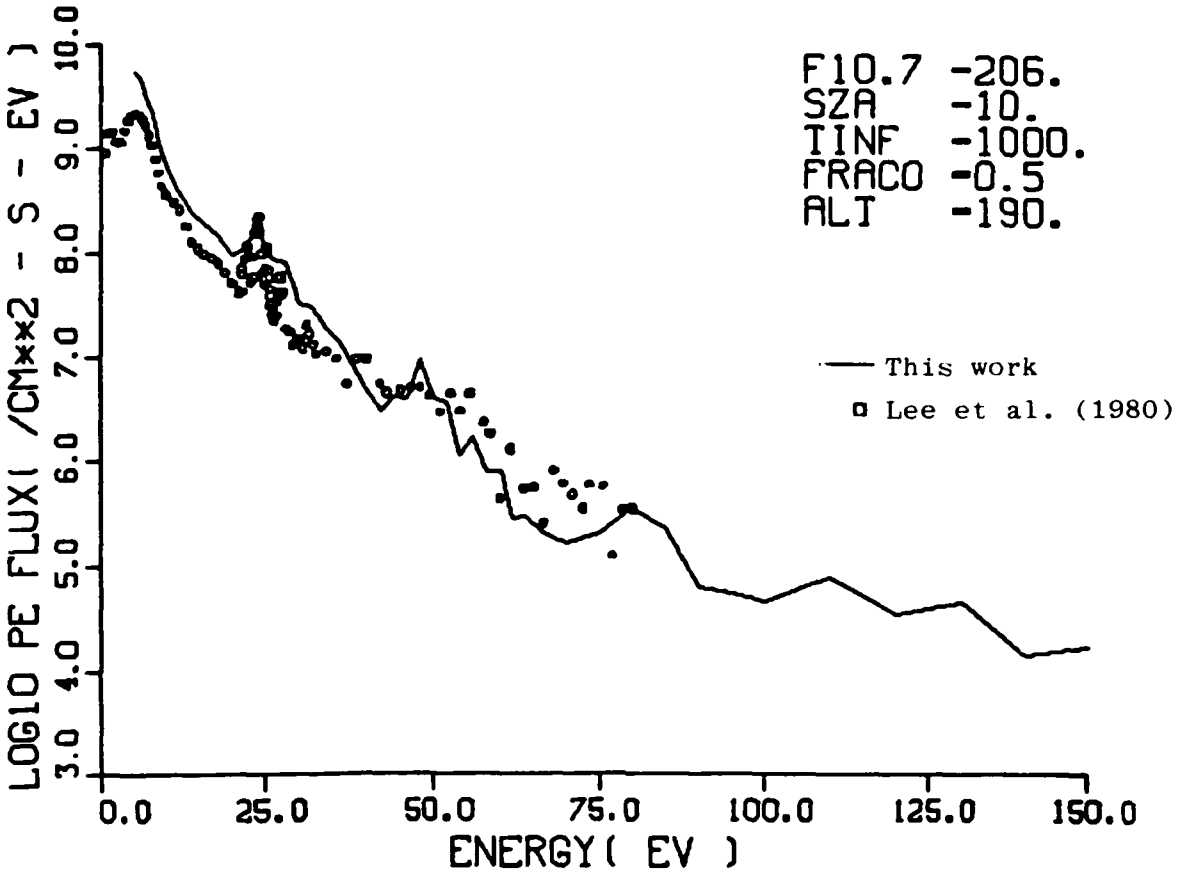

Fig. 3. 4π integrated photoelectron flux. The Lee data are the same as those appearing in Figure 2. The calculated flux is for high solar activity.

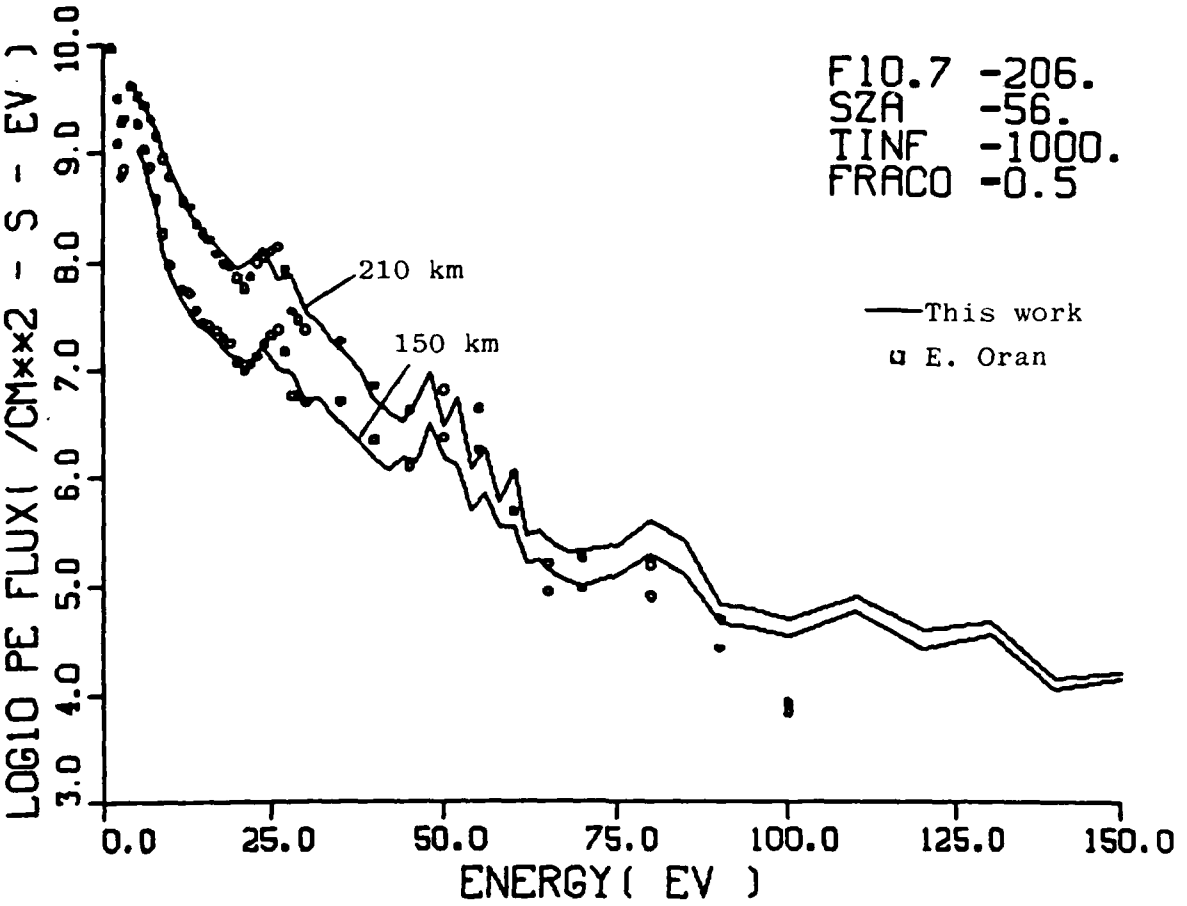

Fig. 4. Comparison of photoelectron fluxes with Oran (private communication) for similar solar and atmospheric conditions.

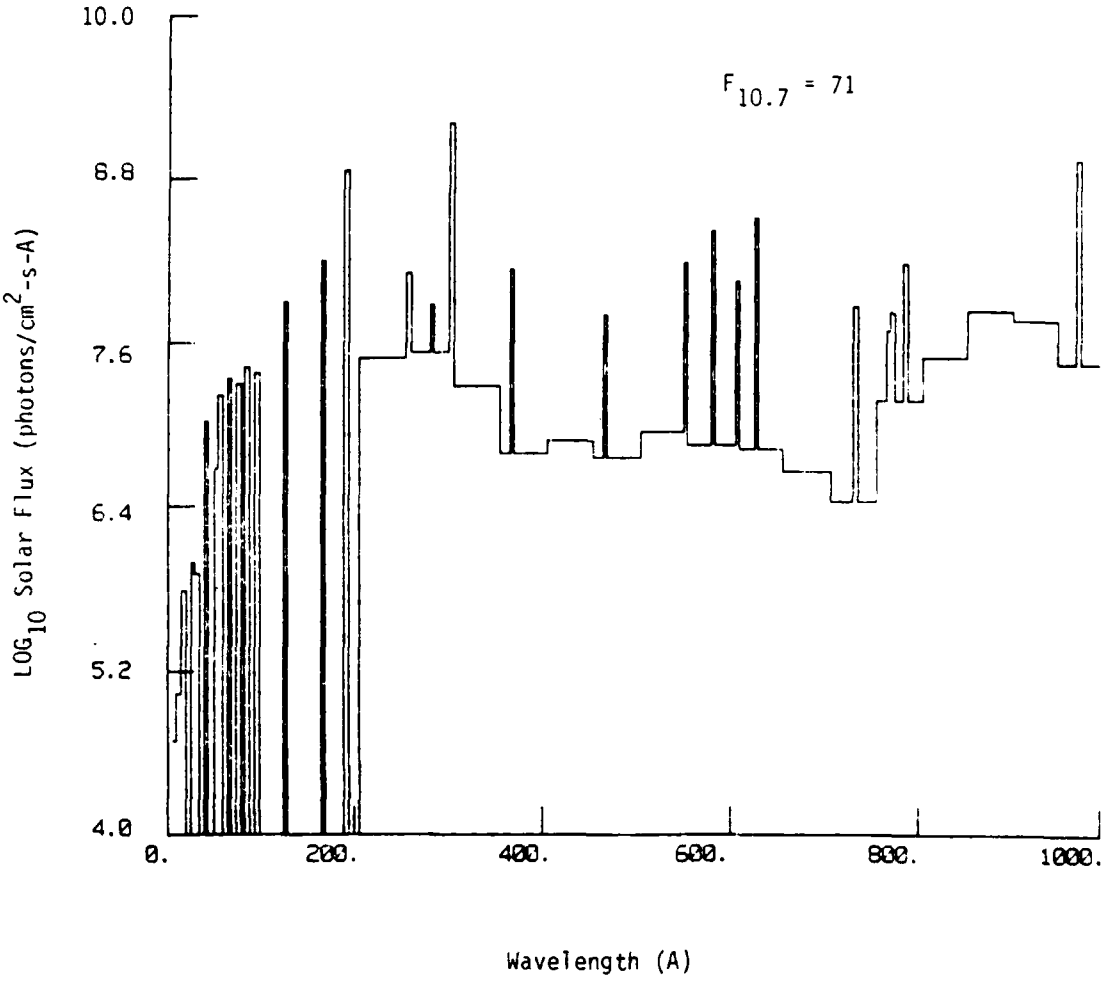

Fig. 5. Representation of solar spectrum for low solar activity. Lines have been given a rectangular distribution with a 5 Å width. The spectrum between 200 and 1000 Å is from Torr et al. (1979) who have associated with it a 10.7 cm solar flux value of 71. The spectrum below 200 Å comes from Donnelly and Pope (1973).

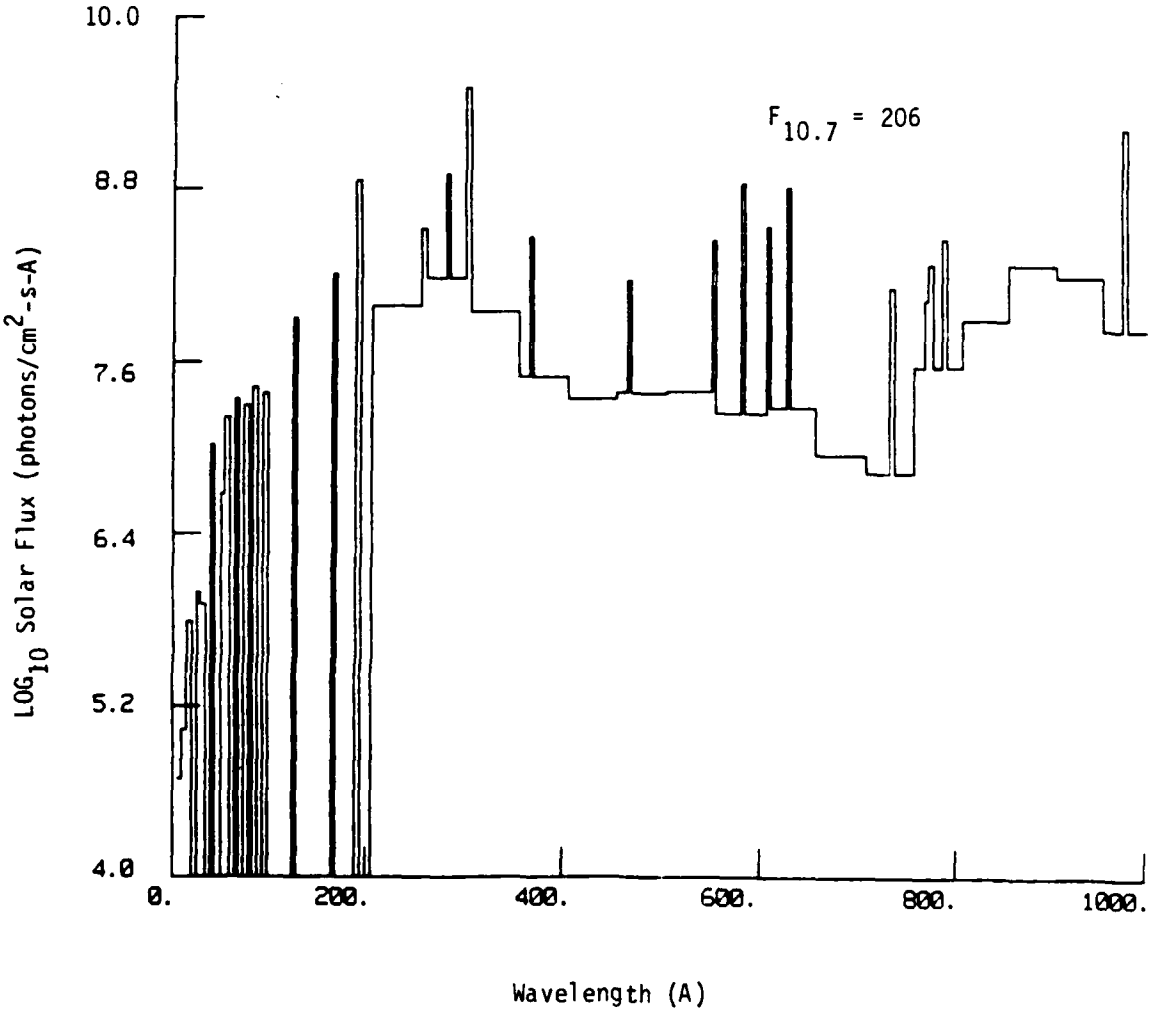

Fig. 6. Similar to Figure 5 except for higher solar activity. Torr et al. (1979) associate with this spectrum a 10.7 cm solar flux value of 206. The spectrum below 200 Å is the same as appears in Figure 5.

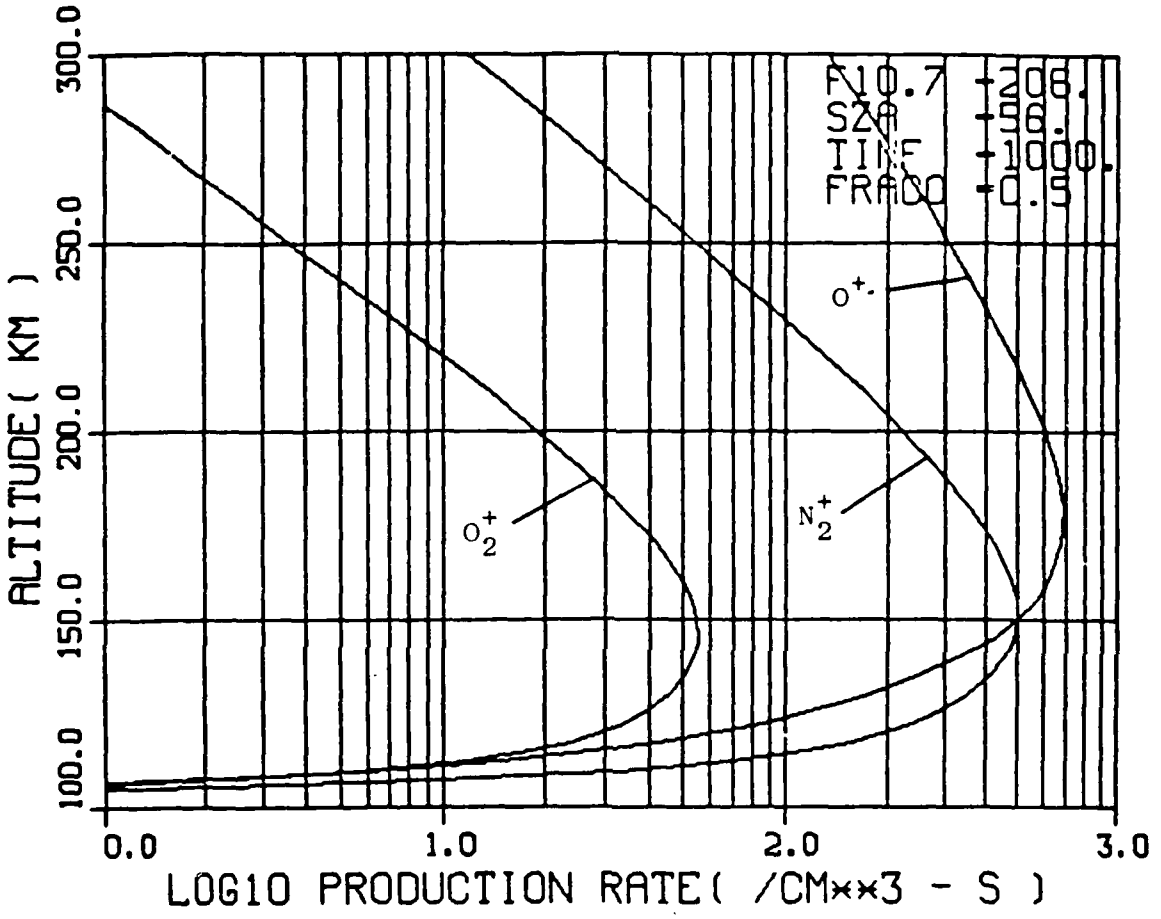

Fig. 7. Calculated ionization rates for conditions identified in the figure.

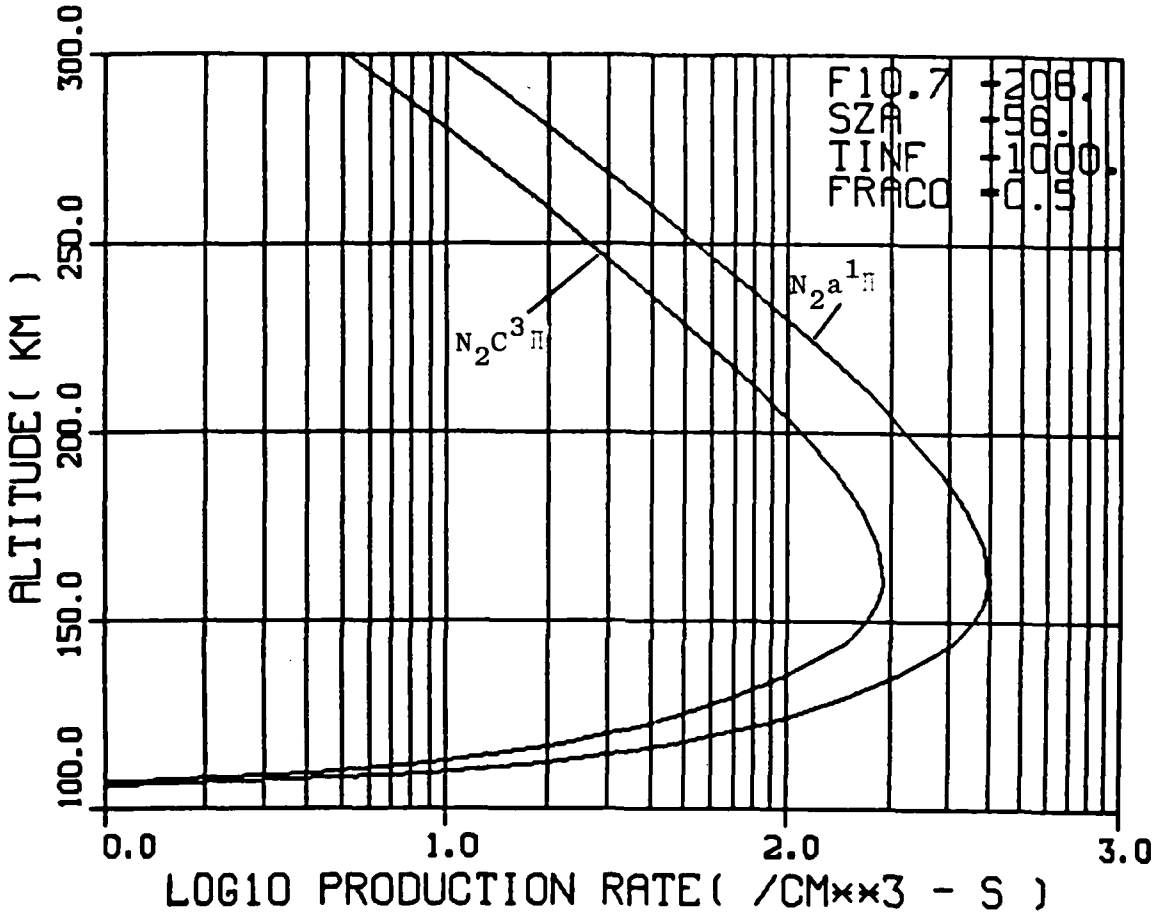

Fig. 8. Excitation rates for the $C^3\Pi$ and $a^1\Pi$ states of N_2. These lead to the second positive and LBH emissions.

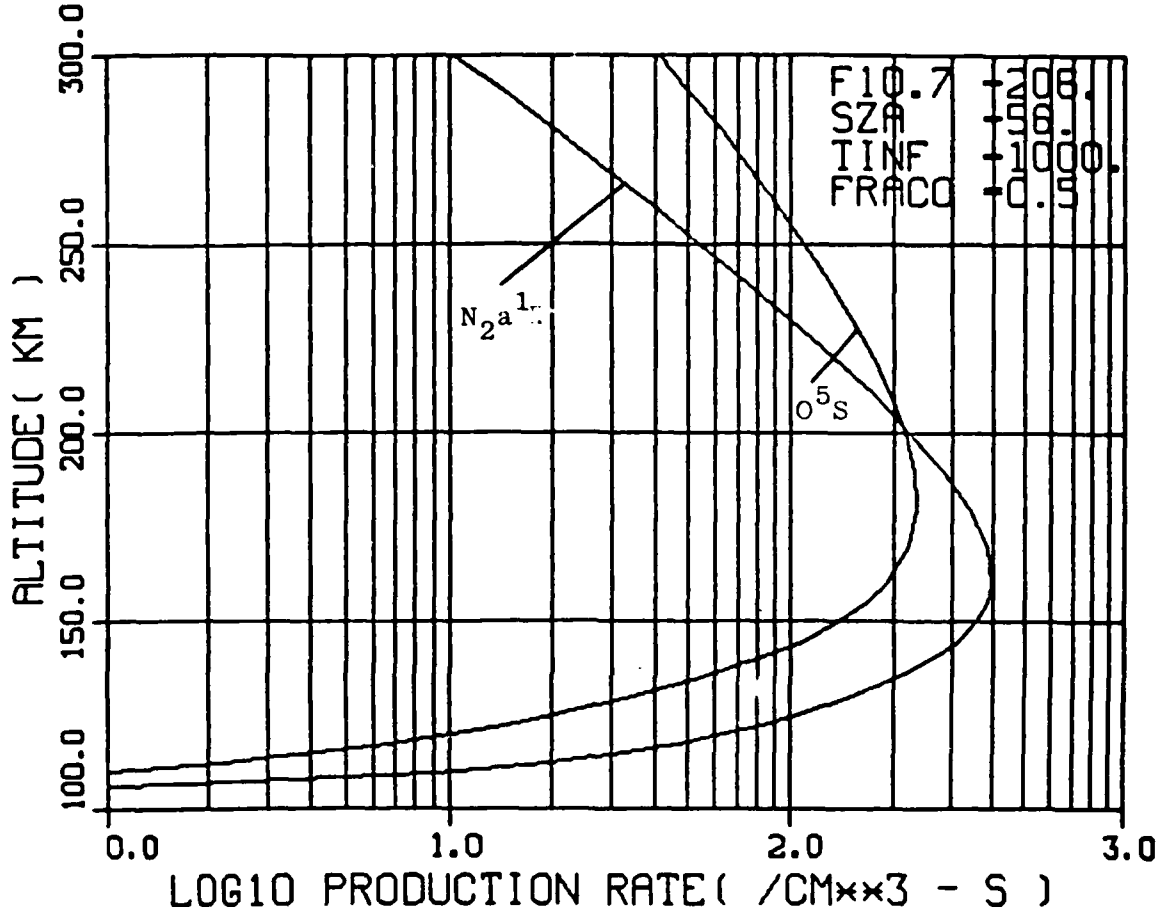

Fig. 9. Excitation rates of the N_2 $a^1\Pi$ state and O^5S state. The ^5S state leads to 1356 Å emission.

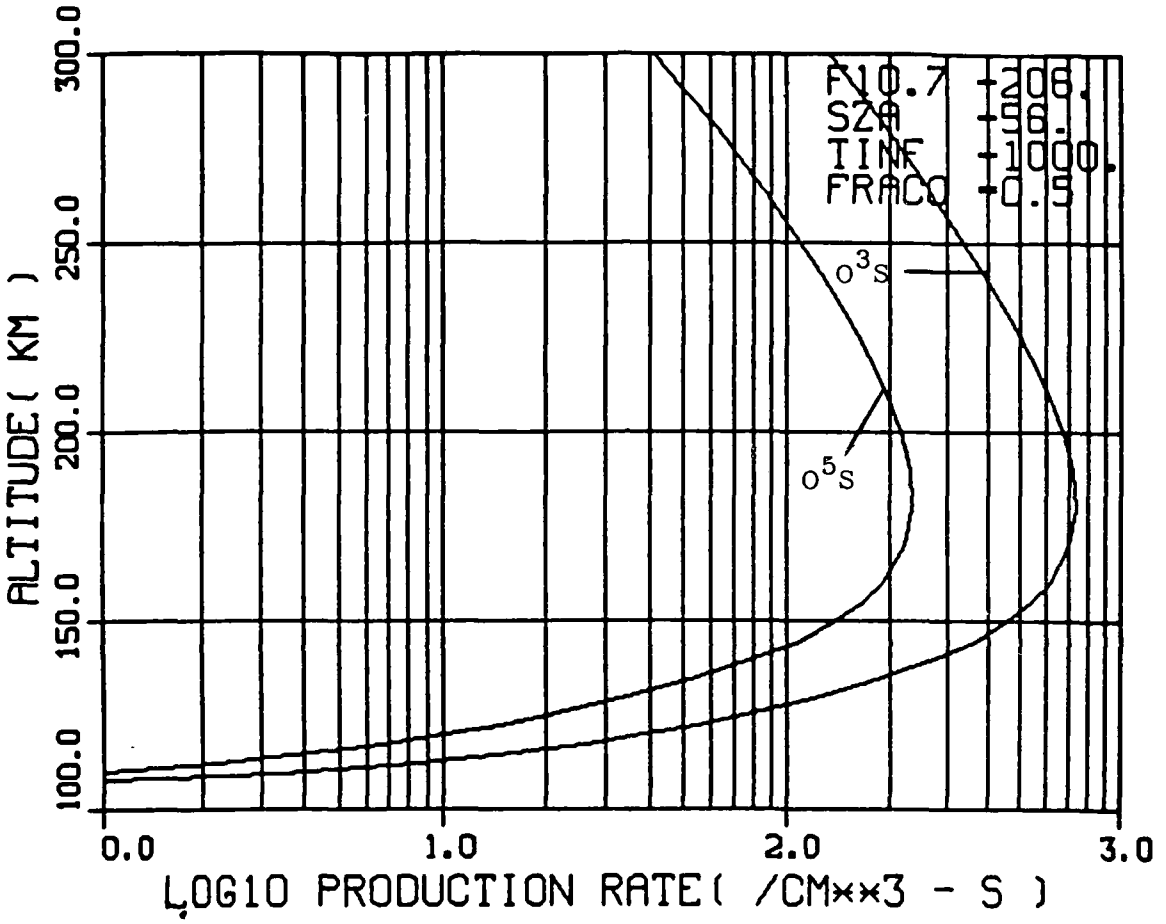

Fig. 10. Excitation rates for the ^5S and ^3S states of O leading to 1356 Å and 1304 Å emission.

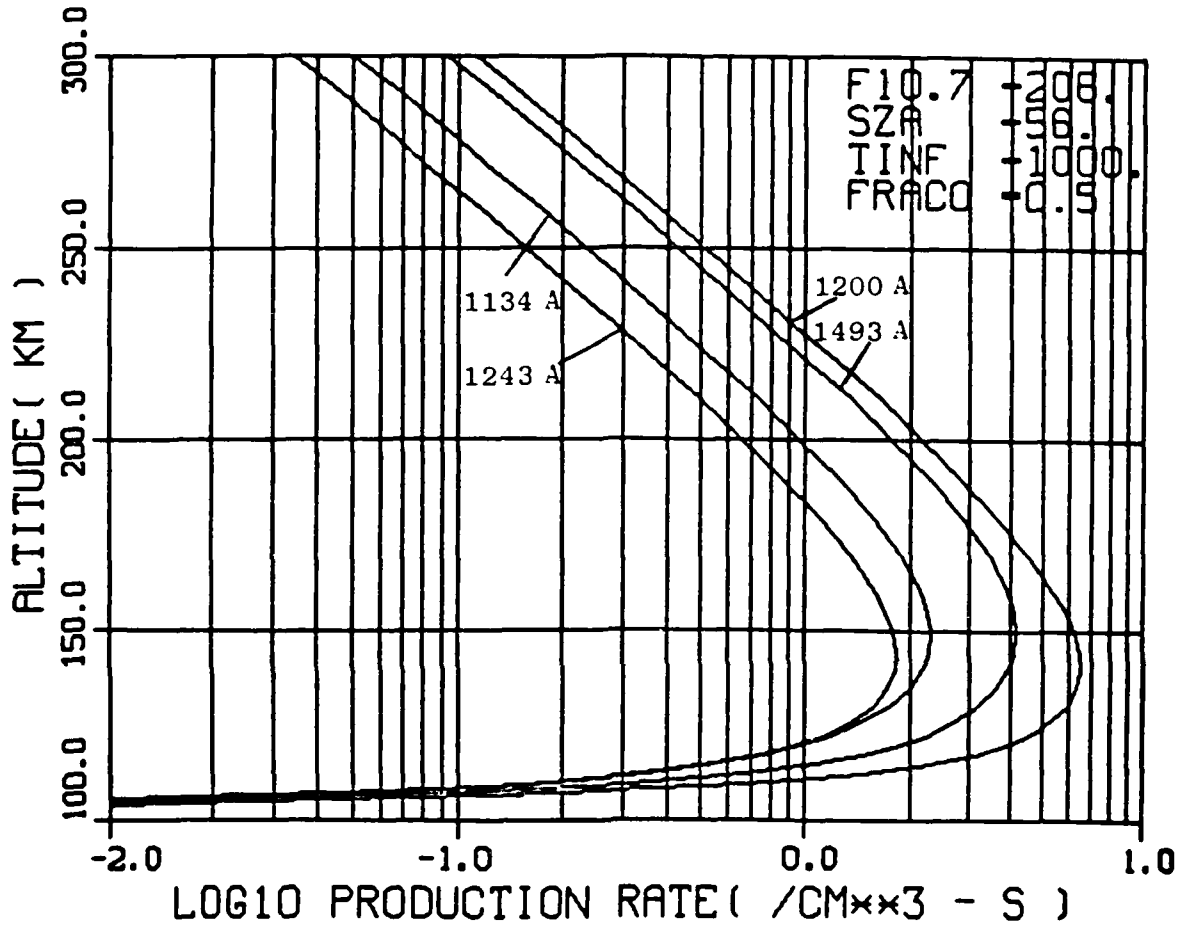

Fig. 11. Emission rates for NI produced by dissociative excitation of N_2.

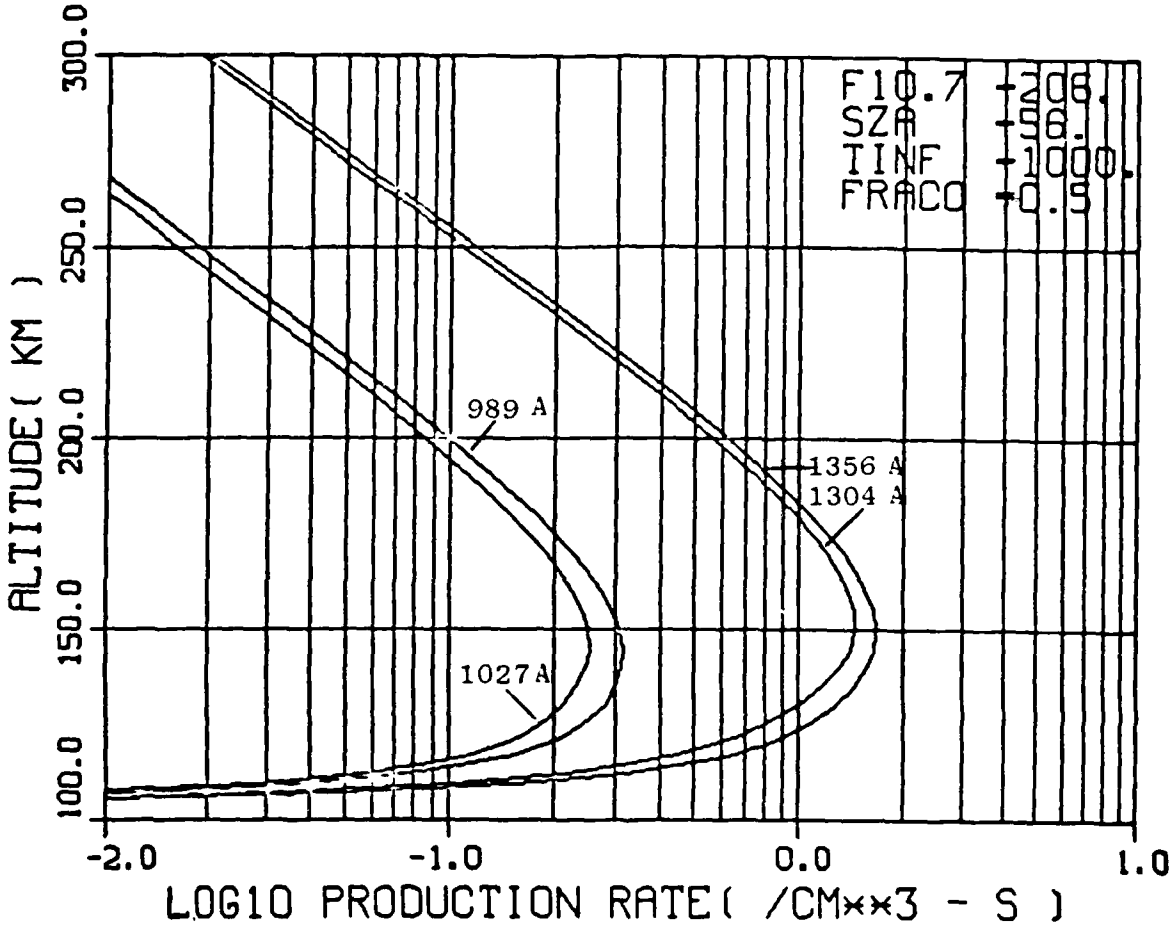

Fig. 12. Emission rates for OI produced by dissociative excitation of O_2.

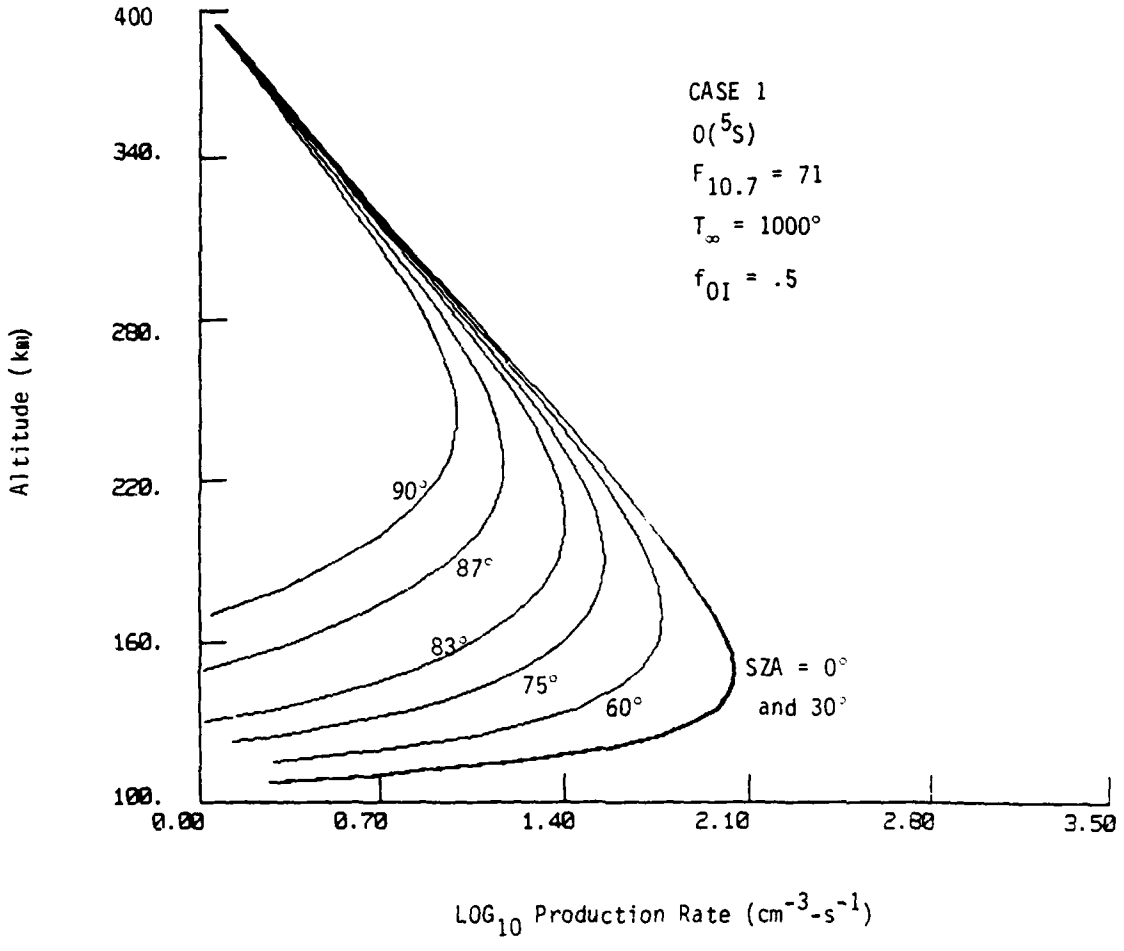

Fig. 13. $O(^5S)$ volume production rate based on the solar spectrum in Figure 5. The parameter f_{OI} scales the Jacchia 1971 atomic oxygen density. SZA refers the solar zenith angle.

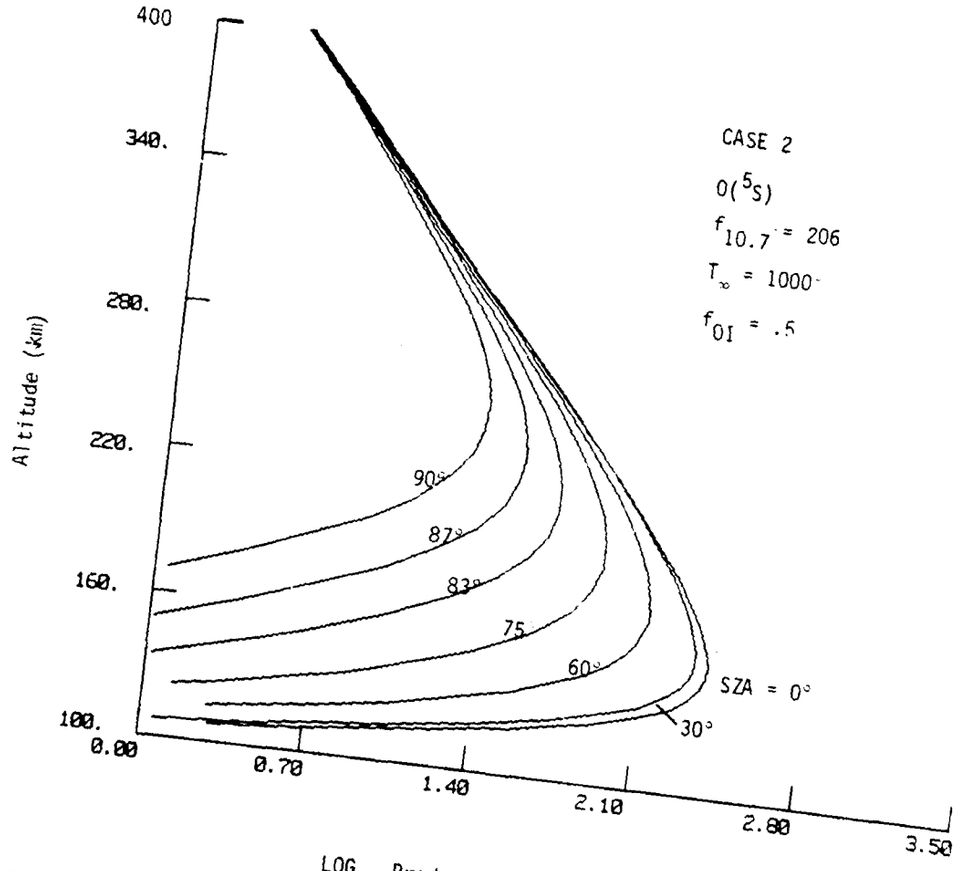

Fig. 14. Similar to Figure 13 except that these rates are based on the solar spectrum in Figure 6.

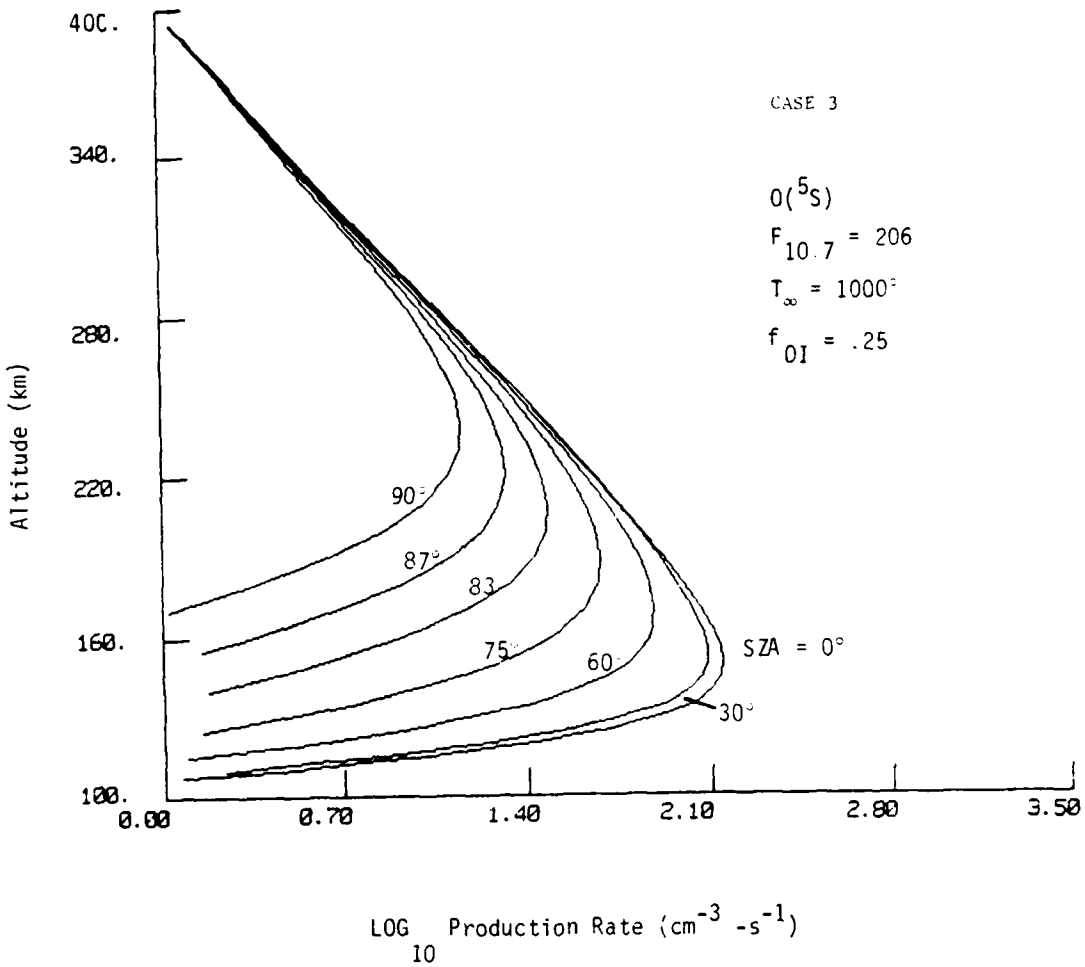

Fig. 15. Similar to Figure 13 except that these rates are based on an O density scaling factor of .25.

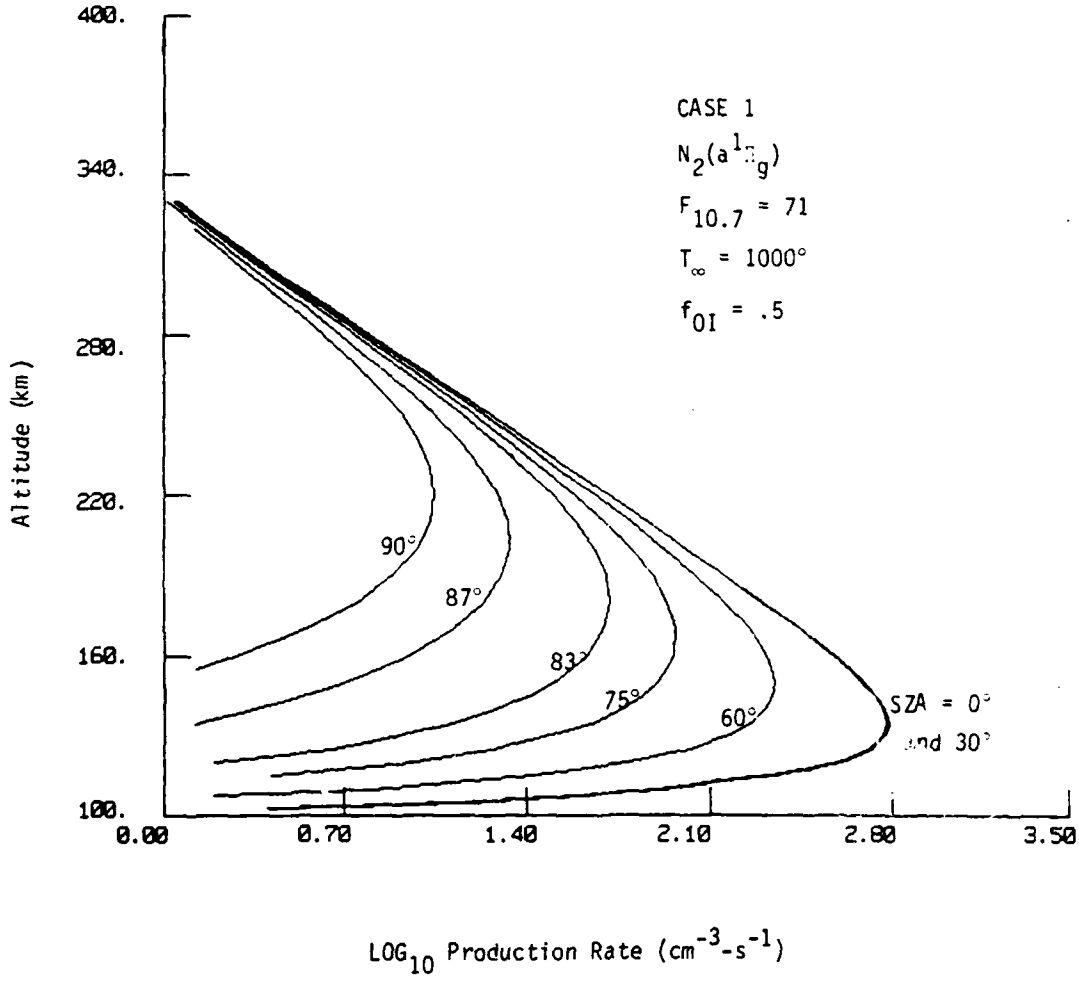

Fig. 16. Similar to Figure 13 except that here the production refers to $N_2(a^1\Pi_g)$.

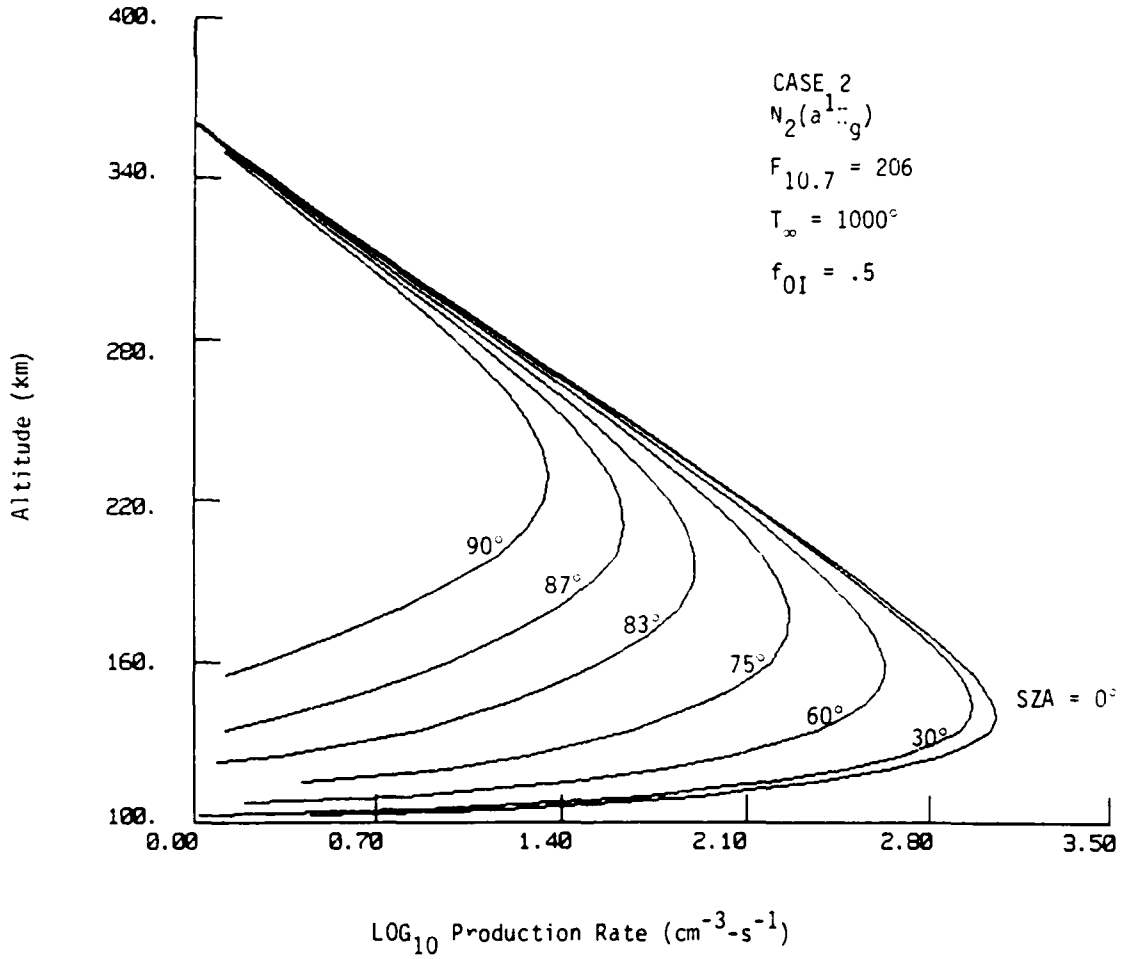

Fig. 17. Similar to Figure 14 except here the production refers to $N_2(a^1\Pi_g)$.

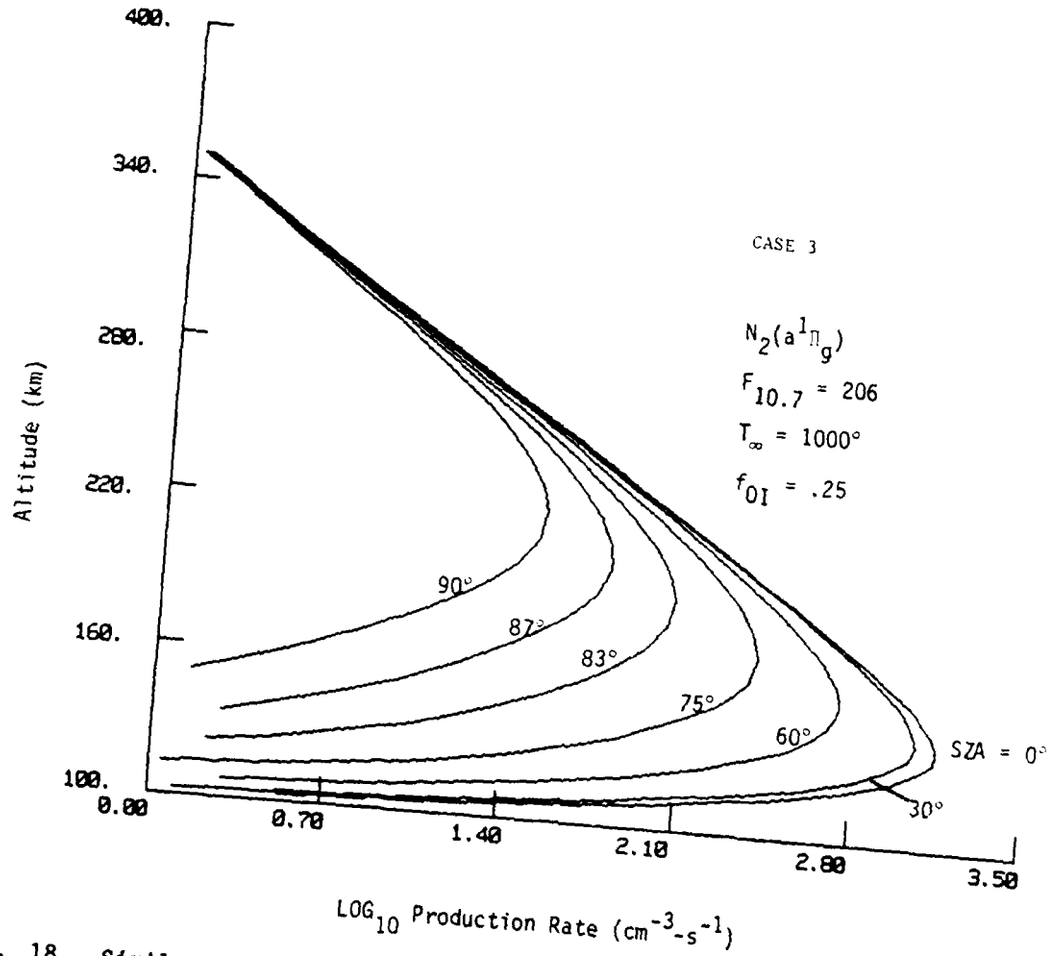

Fig. 18. Similar to Figure 15 except here the production refers to $N_2(a^1\Pi_g)$.

APPENDIX

Tables A1-A4 list the various references for inelastic cross sections for N_2, O_2, O, and N. Table A5 is a tabulation of the numerical values of the cross sections used in the computer code. The entries are the species; the number of inelastic cross sections for that species; a line containing (1) i, the number of values of the individual cross section, (2) the threshold energy, and (3) an identifier of the state; a block containing the i energies (in eV); a block containing the i cross sections (in cm^2) at each of those energies. The first cross section for each species refers to total ionization. The line containing the identifier has one additional parameter not found on corresponding lines for the excitation cross sections. This parameter is used in an analytic expression giving the differential behavior of the cross section.

Table A1. Inelastic Cross Sections for N_2

State	Reference
Ionization	Rapp and Englander-Golden (1965)
Vibration	Schulz (1964)
$A^3\Sigma_u^+$	Borst (1972)
$B^3\Pi_g$	Cartwright et al. (1977)
$C^3\Pi_u$	Cartwright et al. (1977)
$W^3\Delta_u$	Cartwright et al. (1977)
$a\ ^1\Pi_g$	Borst (1972)
$b\ ^1\Pi_g$	Zipf and Gorman (1980)
$w\ ^1\Delta_u$	Cartwright et al. (1977)
$a'\ ^1\Sigma_u^-$	Cartwright et al. (1977)
$a''\ ^1\Sigma_g^+$	Cartwright et al. (1977)
Singlet Rydbergs	Green and Stolarski (1972)
Triplet Rydbergs	P. Julienne (1976, private communication)
$b'\ ^1\Sigma_u^+$	Green and Stolarski (1972)
NI $2s2p^4\ ^4P$ (1134 Å)	Stone and Zipf (1973)
NI $2p^23s\ ^4P$ (1200 Å)	Mumma and Zipf (1971b)
NI $2p^23s'\ ^2D$ (1243 Å)	Mumma and Zipf (1971b)
NI $2p^23s\ ^2P$ (1493 Å)	Mumma and Zipf (1971b)
NII $2s2p^3\ ^3D^\circ$ (1085 Å)	McLaughlin (1977)

Table A2. Inelastic Cross Sections for O_2.

State	Reference
Ionization	Watson et al. (1967); Silverman and Lassettre (1957); Kieffer and Dunn (1966); Rapp et al. (1965)
Vibration	Schulz and Dowell (1962); Hake and Phelps (1967); Trajmar et al. (1972); Wong et al. (1973)
$a^1\Delta_g$	Trajmar et al. (1971)
$b^1\Sigma_g^+$	Trajmar et al. (1971)
$A^3\Sigma_u^+$	Watson et al (1967)
$b^3\Sigma_u^-$	Trajmar et al. (1972)
"9.9" Feature	Watson et al. (1967)
Rydbergs	Watson et al. (1967)
OI $2p^3 3s'\ ^3D^\circ$ (989 Å)	Zipf et al. (1979)
OI $2p^3 3d\ ^3D^\circ$ (1027 Å)	Zipf et al. (1979)
OI $2p^3 3s\ ^3S^\circ$ (1304 Å)	Mumma and Zipf (1971a)
OI $2p^3 3s\ ^5S^\circ$ (1356 Å)	Wells et al. (1971)

Table A3. Inelastic Cross Sections for O.

State	Reference
Ionization	Fite and Brackmann (1959)
$2p^3\ {}^1D$ (6300 Å)	Henry et al. (1969)
$2p^4\ {}^1S$ (5577 Å)	Henry et al. (1969)
$2p^3 3s\ {}^5S^\circ$ (1356 Å)	Stone and Zipf (1974)
$2p^3 3s\ {}^3S^\circ$ (1304 Å)	Stone and Zipf (1974)
(3s) ^3D Rydberg	Davis and Blaha (1976)
(3s) ^1D Rydberg	Davis and Blaha (1976)
OII ^4P	Peach (1971)
OII ^2P	Peach (1971)

Table A4. Inelastic Cross Sections for N

State	Reference
$2s2p^4\ {}^4P$ (1134 Å)	Stone and Zipf (1973)
$2p^2 3s\ {}^4P$ (1200 Å)	Stone and Zipf (1973)
$2p^2\ {}^3s'\ {}^2D$ (1243 Å	Stone and Zipf (1973)
$2p^2 3s\ {}^2P$ (1493 Å)	Stone and Zipf (1973)
$2p^2 3s\ {}^2P$ (1744 Å)	Stone and Zipf (1973)

Table A5. Cross sections

```
N2
42 1.56E+01 1.14E+01 N2 ION
1.56E+01 1.60E+01 1.65E+01 1.70E+01 1.80E+01 1.90E+01 2.00E+01 2.10E+01
2.30E+01 2.50E+01 2.80E+01 3.20E+01 4.00E+01 5.00E+01 6.00E+01 7.00E+01
8.50E+01 1.00E+02 1.25E+02 1.50E+02 2.00E+02 3.00E+02 4.00E+02 6.00E+02
8.00E+02 1.00E+03 1.30E+03 1.70E+03 2.30E+03 3.00E+03 4.00E+03 5.50E+03
7.50E+03 1.00E+04 1.40E+04 2.00E+04 2.50E+04 3.00E+04 4.00E+04 5.00E+04
7.50E+04 1.00E+05
1.00E-19 2.10E-18 4.66E-18 7.13E-18 1.29E-17 1.99E-17 2.70E-17 3.43E-17
4.92E-17 6.40E-17 8.75E-17 1.15E-16 1.57E-16 1.93E-16 2.18E-16 2.33E-16
2.45E-16 2.50E-16 2.52E-16 2.48E-16 2.27E-16 1.92E-16 1.66E-16 1.28E-16
1.07E-16 9.10E-17 7.50E-17 6.00E-17 4.70E-17 3.80E-17 3.00E-17 2.33E-17
1.80E-17 1.42E-17 1.08E-17 8.10E-18 6.80E-18 5.85E-18 4.65E-18 3.90E-18
2.80E-18 2.20E-18
47 0.30 N2 V=1
3.00E-01 7.00E-01 1.10E+00 1.40E+00 1.70E+00 1.80E+00 1.88E+00 1.94E+00
1.98E+00 2.04E+00 2.08E+00 2.12E+00 2.16E+00 2.18E+00 2.22E+00 2.25E+00
2.28E+00 2.32E+00 2.36E+00 2.40E+00 2.44E+00 2.48E+00 2.52E+00 2.58E+00
2.62E+00 2.64E+00 2.66E+00 2.68E+00 2.70E+00 2.72E+00 2.76E+00 2.80E+00
2.83E+00 2.86E+00 2.88E+00 2.90E+00 2.92E+00 2.96E+00 3.02E+00 3.08E+00
3.12E+00 3.16E+00 3.24E+00 3.36E+00 3.50E+00 3.70E+00 4.00E+00
6.70E-20 2.60E-19 1.40E-18 5.00E-18 1.00E-17 1.80E-17 3.90E-17 7.00E-17
1.15E-16 1.50E-16 1.15E-16 7.50E-17 5.00E-17 3.90E-17 5.00E-17 8.20E-17
1.20E-16 1.40E-16 1.20E-16 8.80E-17 6.50E-17 5.50E-17 6.10E-17 8.50E-17
1.00E-16 9.00E-17 6.00E-17 3.00E-17 1.80E-17 1.50E-17 1.90E-17 3.60E-17
4.50E-17 3.60E-17 2.60E-17 1.70E-17 1.50E-17 1.70E-17 2.50E-17 3.60E-17
4.00E-17 3.60E-17 3.00E-17 2.40E-17 2.00E-17 1.70E-17 1.00E-17
46 0.60 N2 V=2
6.00E-01 1.00E+00 1.50E+00 1.70E+00 1.80E+00 1.84E+00 1.88E+00 1.94E+00
2.00E+00 2.06E+00 2.12E+00 2.16E+00 2.22E+00 2.26E+00 2.30E+00 2.34E+00
2.36E+00 2.40E+00 2.42E+00 2.44E+00 2.46E+00 2.50E+00 2.54E+00 2.60E+00
2.64E+00 2.66E+00 2.68E+00 2.72E+00 2.74E+00 2.78E+00 2.82E+00 2.88E+00
2.92E+00 2.96E+00 2.98E+00 3.02E+00 3.06E+00 3.08E+00 3.10E+00 3.12E+00
3.16E+00 3.20E+00 3.26E+00 3.34E+00 3.48E+00 3.60E+00
1.00E-25 1.00E-23 1.00E-21 1.00E-19 2.00E-18 7.50E-18 1.65E-17 3.80E-17
7.30E-17 1.05E-16 1.10E-16 9.30E-17 6.30E-17 4.00E-17 2.50E-17 1.60E-17
1.40E-17 1.90E-17 3.50E-17 6.00E-17 8.50E-17 1.00E-16 8.60E-17 5.50E-17
2.60E-17 1.60E-17 1.30E-17 1.90E-17 3.10E-17 4.50E-17 5.30E-17 4.30E-17
3.00E-17 1.70E-17 1.15E-17 9.20E-18 1.20E-17 1.70E-17 2.50E-17 2.90E-17
2.60E-17 2.00E-17 1.45E-17 1.05E-17 7.00E-18 5.50E-18
31 0.90 N2 V=3
9.00E-01 1.20E+00 1.50E+00 1.70E+00 1.80E+00 1.88E+00 1.94E+00 2.00E+00
2.06E+00 2.14E+00 2.20E+00 2.26E+00 2.32E+00 2.36E+00 2.40E+00 2.44E+00
2.48E+00 2.54E+00 2.60E+00 2.66E+00 2.70E+00 2.74E+00 2.78E+00 2.82E+00
2.86E+00 2.92E+00 2.98E+00 3.02E+00 3.06E+00 3.14E+00 3.24E+00
1.00E-23 1.00E-22 1.00E-21 1.00E-20 1.00E-19 2.00E-18 8.50E-18 2.10E-17
4.30E-17 7.50E-17 9.00E-17 7.50E-17 3.60E-17 1.50E-17 1.00E-17 1.50E-17
2.50E-17 4.00E-17 4.80E-17 4.00E-17 2.30E-17 1.20E-17 1.00E-17 1.35E-17
2.10E-17 2.60E-17 2.00E-17 1.20E-17 9.30E-18 9.00E-18 8.50E-18
```

Table A5 (Cont'd) - Cross sections

```
36 1.20 N2 V=4
1.20E+00 1.40E+00 1.60E+00 1.80E+00 1.90E+00 1.95E+00 2.00E+00 2.04E+00
2.08E+00 2.12E+00 2.16E+00 2.22E+00 2.28E+00 2.34E+00 2.40E+00 2.46E+00
2.48E+00 2.50E+00 2.54E+00 2.58E+00 2.62E+00 2.65E+00 2.68E+00 2.72E+00
2.76E+00 2.79E+00 2.82E+00 2.84E+00 2.88E+00 2.92E+00 2.96E+00 3.00E+00
3.06E+00 3.12E+00 3.16E+00 3.20E+00
1.00E-23 1.00E-22 1.00E-21 1.00E-20 1.00E-19 3.00E-19 1.00E-18 4.00E-18
1.00E-17 2.50E-17 4.30E-17 6.30E-17 7.20E-17 6.00E-17 4.00E-17 2.50E-17
1.50E-17 1.00E-17 7.50E-18 8.50E-18 1.40E-17 2.00E-17 3.00E-17 3.80E-17
3.00E-17 1.80E-17 1.00E-17 7.50E-18 5.40E-18 6.00E-18 8.00E-18 1.15E-17
1.30E-17 1.15E-17 8.00E-18 4.00E-18
37 1.50 N2 V=5
1.50E+00 1.70E+00 1.90E+00 2.00E+00 2.06E+00 2.10E+00 2.14E+00 2.20E+00
2.26E+00 2.32E+00 2.38E+00 2.44E+00 2.50E+00 2.54E+00 2.56E+00 2.58E+00
2.60E+00 2.62E+00 2.66E+00 2.70E+00 2.74E+00 2.78E+00 2.82E+00 2.88E+00
2.92E+00 2.96E+00 2.98E+00 3.00E+00 3.04E+00 3.08E+00 3.12E+00 3.16E+00
3.20E+00 3.24E+00 3.28E+00 3.30E+00 3.34E+00
1.00E-23 1.00E-22 1.00E-21 3.00E-19 2.50E-18 7.50E-18 1.50E-17 2.50E-17
3.30E-17 4.00E-17 4.60E-17 5.00E-17 4.50E-17 3.30E-17 2.10E-17 9.50E-18
5.00E-18 3.00E-18 3.50E-18 6.10E-18 1.00E-17 1.50E-17 2.05E-17 2.25E-17
2.10E-17 1.20E-17 5.00E-18 3.00E-18 3.00E-18 4.30E-18 7.50E-18 1.00E-17
1.10E-17 9.50E-18 5.00E-18 3.00E-18 1.00E-18
25 1.80 N2 V=6
1.80E+00 1.90E+00 2.00E+00 2.10E+00 2.20E+00 2.25E+00 2.28E+00 2.30E+00
2.32E+00 2.36E+00 2.40E+00 2.46E+00 2.52E+00 2.58E+00 2.64E+00 2.70E+00
2.78E+00 2.84E+00 2.90E+00 2.96E+00 3.00E+00 3.04E+00 3.10E+00 3.16E+00
3.20E+00
1.00E-24 1.00E-23 1.00E-22 1.00E-21 1.00E-20 1.00E-19 5.00E-19 1.50E-18
6.00E-18 2.00E-17 3.40E-17 4.90E-17 5.40E-17 4.90E-17 3.50E-17 2.10E-17
1.05E-17 9.00E-18 1.05E-17 1.30E-17 1.35E-17 1.10E-17 6.00E-18 3.10E-18
1.50E-18
31 2.10 N2 V=7
2.10E+00 2.20E+00 2.30E+00 2.36E+00 2.40E+00 2.42E+00 2.46E+00 2.52E+00
2.58E+00 2.64E+00 2.68E+00 2.74E+00 2.78E+00 2.82E+00 2.84E+00 2.86E+00
2.88E+00 2.90E+00 2.92E+00 2.96E+00 3.00E+00 3.02E+00 3.04E+00 3.06E+00
3.10E+00 3.16E+00 3.22E+00 3.28E+00 3.32E+00 3.36E+00 3.40E+00
1.00E-22 1.00E-21 1.00E-20 1.00E-19 1.50E-18 4.70E-18 9.00E-18 1.40E-17
1.80E-17 2.50E-17 3.00E-17 2.60E-17 1.80E-17 1.60E-17 1.30E-17 8.00E-18
5.20E-18 3.40E-18 2.40E-18 1.70E-18 1.50E-18 2.20E-18 3.40E-18 4.80E-18
6.60E-18 7.50E-18 7.10E-18 5.50E-18 3.50E-18 2.00E-18 1.00E-18
25 2.40 N2 V=8
2.40E+00 2.45E+00 2.50E+00 2.53E+00 2.56E+00 2.58E+00 2.60E+00 2.64E+00
2.70E+00 2.76E+00 2.82E+00 2.88E+00 2.94E+00 2.98E+00 3.02E+00 3.06E+00
3.10E+00 3.14E+00 3.18E+00 3.22E+00 3.26E+00 3.30E+00 3.34E+00 3.38E+00
3.40E+00
1.00E-22 1.00E-21 1.00E-20 1.00E-19 1.50E-18 3.20E-18 5.50E-18 9.50E-18
1.25E-17 1.30E-17 1.20E-17 1.00E-17 7.00E-18 5.00E-18 2.50E-18 1.40E-18
1.30E-18 1.40E-18 1.80E-18 2.90E-18 4.00E-18 4.50E-18 3.80E-18 2.40E-18
1.50E-18
19 6.17 N2 A3SIG
6.50E+00 7.00E+00 7.50E+00 8.00E+00 9.00E+00 1.00E+01 1.10E+01 1.20E+01
1.30E+01 1.50E+01 1.70E+01 2.00E+01 2.50E+01 3.00E+01 4.00E+01 5.00E+01
6.00E+01 7.50E+01 1.00E+02
5.00E-19 2.00E-18 5.00E-18 1.50E-17 2.60E-17 4.00E-17 5.00E-17 4.30E-17
3.30E-17 2.30E-17 1.70E-17 1.30E-17 8.50E-18 5.80E-18 3.00E-18 1.60E-18
1.10E-18 6.00E-19 3.00E-19
```

Table A5 (Cont'd) - Cross sections

```
11 7.35 N2 B3PI
 .40E+00 7.50E+00 7.70E+00 8.00E+00 8.50E+00 9.00E+00 1.00E+01 1.10E+01
 .20E+01 1.30E+01 1.40E+01 1.60E+01 2.00E+01 2.60E+01 3.50E+01 4.50E+01
 .00E+01 8.00E+01 1.10E+02 1.50E+02 2.00E+02
1.00E-19 4.00E-19 1.00E-18 5.00E-18 9.00E-18 1.50E-17 2.20E-17 2.80E-17
 .00E-17 3.00E-17 2.70E-17 2.10E-17 1.60E-17 1.20E-17 7.80E-18 4.40E-19
1.80E-18 7.80E-19 3.00E-19 1.20E-19 5.00E-20
20 11.0 N2 C3PI
 .13E+01 1.15E+01 1.20E+01 1.25E+01 1.30E+01 1.35E+01 1.40E+01 1.45E+01
 .50E+01 1.60E+01 1.70E+01 1.80E+01 2.00E+01 2.50E+01 3.00E+01 4.00E+01
5.00E+01 7.50E+01 1.00E+02 2.00E+02
1.00E-18 2.50E-18 6.50E-18 1.10E-17 2.10E-17 3.30E-17 4.10E-17 4.00E-17
3.40E-17 2.70E-17 2.30E-17 2.00E-17 1.50E-17 9.40E-18 6.80E-18 3.80E-18
2.10E-18 6.50E-19 2.70E-19 3.40E-20
13 7.50 N2 W3DEL
7.50E+00 7.60E+00 7.70E+00 7.80E+00 8.00E+00 8.30E+00 8.60E+00 9.00E+00
1.00E+01 1.10E+01 1.30E+01 1.50E+01 1.65E+01 1.80E+01 2.10E+01 2.50E+01
3.20E+01 4.00E+01 5.50E+01 7.50E+01 1.00E+02 1.50E+02 2.00E+02
1.00E-19 3.00E-19 7.00E-19 1.00E-18 2.00E-18 4.00E-18 5.50E-18 7.40E-18
1.20E-17 1.70E-17 2.60E-17 3.60E-17 3.80E-17 3.50E-17 2.20E-17 1.40E-17
8.40E-18 5.00E-18 1.90E-18 7.60E-19 3.20E-19 9.50E-20 4.00E-20
30 8.55 N2 A1PI
9.00E+00 9.50E+00 1.00E+01 1.10E+01 1.20E+01 1.30E+01 1.40E+01 1.50E+01
1.60E+01 1.70E+01 1.90E+01 2.20E+01 2.50E+01 3.00E+01 4.00E+01 6.00E+01
9.00E+01 1.25E+02 1.50E+02 2.00E+02 3.00E+02 5.00E+02 7.50E+02 1.00E+03
1.50E+03 2.00E+03 3.00E+03 5.00E+03 7.50E+03 1.00E+04
1.50E-18 4.90E-18 8.50E-18 1.50E-17 2.20E-17 2.90E-17 3.40E-17 3.70E-17
3.85E-17 3.80E-17 3.50E-17 3.16E-17 2.80E-17 2.35E-17 1.75E-17 1.15E-17
7.70E-18 5.50E-18 4.60E-18 3.45E-18 2.30E-18 1.38E-18 9.20E-19 6.90E-19
4.60E-19 3.45E-19 2.30E-19 1.38E-19 9.20E-20 6.90E-20
17 13.0 N2 B1PIU
1.30E+01 1.35E+01 1.45E+01 1.65E+01 2.10E+01 3.20E+01 5.50E+01 1.00E+02
1.90E+02 5.00E+02 1.00E+03 1.90E+03 4.00E+03 9.00E+03 2.10E+04 4.50E+04
1.00E+05
2.30E-18 5.00E-18 1.18E-17 2.30E-17 3.85E-17 4.65E-17 4.30E-17 3.20E-17
2.10E-17 1.15E-17 7.00E-18 4.20E-18 2.30E-18 1.20E-18 5.85E-19 3.00E-19
1.50E-19
12 10.0 N2 W1DEL
1.00E+01 1.35E+01 1.50E+01 2.00E+01 2.50E+01 3.00E+01 4.00E+01 5.00E+01
6.00E+01 8.00E+01 1.00E+02 1.40E+02
4.00E-18 1.20E-17 1.00E-17 4.35E-18 3.00E-18 2.28E-18 1.30E-18 8.25E-19
5.70E-19 3.20E-19 2.05E-19 1.00E-19
15 10.0 N2 A'
1.00E+01 1.40E+01 1.50E+01 2.00E+01 2.50E+01 3.00E+01 4.00E+01 5.00E+01
6.00E+01 8.00E+01 1.00E+02 1.50E+02 2.00E+02 4.00E+02 8.80E+02
3.00E-18 1.00E-17 9.50E-18 4.95E-18 3.50E-18 2.90E-18 2.25E-18 1.78E-18
1.50E-18 1.10E-18 8.90E-19 5.90E-19 4.40E-19 2.20E-19 1.00E-19
15 12.5 N2 A''
1.25E+01 1.50E+01 1.95E+01 2.00E+01 2.50E+01 3.00E+01 4.00E+01 5.00E+01
6.00E+01 8.00E+01 1.00E+02 1.50E+02 2.00E+02 4.00E+02 6.70E+02
1.00E-18 3.50E-18 5.95E-18 5.80E-18 3.65E-18 2.60E-18 1.75E-18 1.37E-18
1.13E-18 8.50E-19 6.75E-19 4.50E-19 3.35E-19 1.70E-19 1.00E-19
16 13.0 N2 3RYD
1.30E+01 1.40E+01 1.50E+01 1.70E+01 2.00E+01 2.25E+01 2.50E+01 3.00E+01
3.50E+01 4.00E+01 5.00E+01 7.00E+01 9.00E+01 1.20E+02 1.50E+02 2.00E+02
1.00E-18 1.50E-17 2.90E-17 4.30E-17 5.20E-17 5.00E-17 4.50E-17 3.10E-17
1.80E-17 1.23E-17 6.20E-18 2.20E-18 1.10E-18 4.60E-19 2.30E-19 9.60E-20
```

Table A5 (Cont'd) - Cross sections

```
30 13.5 N2 B1SIG
1.35E+01 1.40E+01 1.70E+01 2.00E+01 2.30E+01 2.70E+01 3.20E+01 4.00E+01
5.00E+01 6.00E+01 7.00E+01 8.00E+01 1.00E+02 1.50E+02 2.00E+02 3.00E+02
5.00E+02 7.50E+02 1.00E+03 1.50E+03 2.00E+03 3.00E+03 5.00E+03 7.50E+03
1.00E+04 2.00E+04 3.00E+04 5.00E+04 7.50E+04 1.00E+05
1.00E-20 1.00E-19 7.00E-19 2.00E-18 5.00E-18 8.00E-18 1.07E-17 1.40E-17
1.60E-17 1.65E-17 1.68E-17 1.67E-17 1.60E-17 1.40E-17 1.20E-17 9.60E-
6.90E-18 5.20E-18 4.20E-18 3.00E-18 2.40E-18 1.70E-18 1.12E-18 8.00E-1
6.30E-19 3.50E-19 2.50E-19 1.60E-19 1.10E-19 8.50E-20
28 16.0 N2 1RYD
1.60E+01 1.70E+01 1.80E+01 2.00E+01 2.50E+01 3.00E+01 4.00E+01 5.00E+01
7.50E+01 1.00E+02 1.50E+02 2.00E+02 3.00E+02 5.00E+02 7.50E+02 1.00E+03
1.50E+03 2.00E+03 3.00E+03 5.00E+03 7.50E+03 1.00E+04 1.50E+04 2.00E+04
3.00E+04 5.00E+04 7.50E+04 1.00E+05
2.20E-18 5.50E-18 1.00E-17 2.10E-17 5.00E-17 7.80E-17 1.15E-16 1.33E-16
1.40E-16 1.32E-16 1.13E-16 9.80E-17 7.90E-17 5.70E-17 4.40E-17 3.60E-17
2.70E-17 2.20E-17 1.60E-17 1.10E-17 7.60E-18 6.00E-18 4.25E-18 3.40E-18
2.40E-18 1.55E-18 1.10E-18 8.70E-19
23 20.0 NI 1134
2.00E+01 2.50E+01 3.00E+01 3.50E+01 4.00E+01 4.40E+01 5.00E+01 5.70E+01
6.00E+01 7.00E+01 8.00E+01 9.00E+01 1.00E+02 1.20E+02 1.40E+02 1.60E+02
1.80E+02 2.00E+02 2.20E+02 2.40E+02 2.60E+02 2.80E+02 3.00E+02
1.24E-20 2.48E-19 6.45E-19 7.44E-19 7.81E-19 7.94E-19 1.08E-18 1.24E-18
1.25E-18 1.25E-18 1.24E-18 1.22E-18 1.20E-18 1.14E-18 1.06E-18 9.73E-19
9.11E-19 8.68E-19 8.12E-19 7.68E-19 7.25E-19 6.88E-19 6.63E-19
24 20.1 NI 1200
2.50E+01 2.75E+01 3.00E+01 3.25E+01 3.50E+01 3.75E+01 4.00E+01 4.25E+01
4.50E+01 4.75E+01 5.00E+01 6.00E+01 7.00E+01 8.00E+01 9.00E+01 1.00E+02
1.25E+02 1.50E+02 1.75E+02 2.00E+02 2.25E+02 2.50E+02 2.75E+02 3.00E+02
5.30E-19 1.00E-18 1.37E-18 1.71E-18 1.84E-18 1.97E-18 2.01E-18 2.35E-18
2.78E-18 3.22E-18 3.69E-18 5.30E-18 6.35E-18 6.70E-18 6.75E-18 6.70E-18
6.30E-18 5.87E-18 5.49E-18 5.11E-18 4.75E-18 4.43E-18 4.15E-18 3.98E-18
25 22.5 NI 1243
2.25E+01 2.50E+01 2.75E+01 3.00E+01 3.25E+01 3.50E+01 3.75E+01 4.00E+01
4.25E+01 4.50E+01 4.75E+01 5.00E+01 6.00E+01 7.00E+01 8.00E+01 9.00E+01
1.00E+02 1.25E+02 1.50E+02 1.75E+02 2.00E+02 2.25E+02 2.50E+02 2.75E+02
3.00E+02
5.80E-20 9.40E-20 2.90E-19 4.06E-19 5.08E-19 5.73E-19 6.30E-19 6.81E-19
7.18E-19 8.12E-19 8.99E-19 9.90E-19 1.35E-18 1.52E-18 1.54E-18 1.52E-18
1.45E-18 1.33E-18 1.20E-18 1.09E-18 9.90E-19 9.20E-19 8.50E-19 7.80E-19
7.20E-19
25 22.5 NI 1493
2.25E+01 2.50E+01 2.75E+01 3.00E+01 3.25E+01 3.50E+01 3.75E+01 4.00E+01
4.25E+01 4.50E+01 4.75E+01 5.00E+01 6.00E+01 7.00E+01 8.00E+01 9.00E+01
1.00E+02 1.25E+02 1.50E+02 1.75E+02 2.00E+02 2.25E+02 2.50E+02 2.75E+02
3.00E+02
4.19E-19 6.34E-19 8.51E-19 9.56E-19 1.00E-18 1.02E-18 1.03E-18 1.19E-18
1.47E-18 1.59E-18 1.79E-18 1.89E-18 2.39E-18 2.68E-18 2.68E-18 2.68E-18
2.62E-18 2.51E-18 2.35E-18 2.15E-18 1.98E-18 1.86E-18 1.73E-18 1.60E-18
1.52E-18
16 36.  NII 1085
3.60E+01 4.00E+01 4.50E+01 5.20E+01 6.00E+01 7.50E+01 9.00E+01 1.10E+02
1.30E+02 1.60E+02 2.00E+02 2.60E+02 3.50E+02 5.50E+02 8.00E+02 1.20E+03
1.00E-20 2.10E-19 7.00E-19 1.50E-18 2.20E-18 2.90E-18 3.40E-18 4.00E-18
4.20E-18 4.20E-18 3.90E-18 3.10E-18 2.20E-18 1.40E-18 9.40E-19 9.40E-19
```

Table A5 (Cont'd) - Cross sections

```
 1.25E+01 1.52E+01 02 ION
1.25E+01 1.30E+01 1.40E+01 1.50E+01 1.70E+01 2.00E+01 2.50E+01 3.00E+01
4.00E+01 5.00E+01 7.00E+01 1.00E+02 1.25E+02 1.50E+02 2.00E+02 3.00E+02
4.00E+02 5.00E+02 7.00E+02 1.00E+03 1.50E+03 2.00E+03 3.00E+03 5.00E+03
7.50E+03 1.00E+04 1.50E+04 2.50E+04 5.00E+04
1.00E-18 2.30E-18 5.50E-18 8.50E-18 1.80E-17 3.10E-17 6.20E-17 9.30E-17
1.45E-16 1.90E-16 2.40E-16 2.70E-16 2.75E-16 2.70E-16 2.40E-16 2.00E-16
1.70E-16 1.47E-16 1.17E-16 9.00E-17 6.70E-17 5.30E-17 3.90E-17 2.60E-17
1.87E-17 1.40E-17 1.05E-17 7.00E-18 3.70E-18
29 0.30 02 VIB
3.00E-01 3.50E-01 3.80E-01 4.00E-01 5.00E-01 7.00E-01 9.00E-01 9.50E-01
1.00E 00 1.20E 00 1.50E 00 2.00E 00 2.50E 00 3.00E 00 4.00E 00 4.50E 00
5.00E 00 6.00E 00 7.00E 00 8.00E 00 9.00E 00 1.00E 01 1.20E 01 1.50E 01
2.00E 01 3.00E 01 4.00E 01 5.00E 01 1.00E 02
9.00E-18 9.50E-18 8.00E-18 7.00E-18 4.20E-18 2.00E-18 1.30E-18 4.00E-18
1.00E-17 1.00E-17 7.00E-18 4.00E-18 2.70E-18 1.60E-18 1.20E-18 4.00E-18
8.00E-18 1.80E-17 3.00E-17 4.40E-17 5.40E-17 5.00E-17 3.00E-17 6.00E-18
4.00E-18 2.20E-18 1.50E-18 1.20E-18 5.00E-19
23 1.20 02 A1DEL
1.20E+00 1.40E+00 1.70E+00 2.00E+00 2.50E+00 3.00E+00 4.00E+00 5.00E+00
6.00E+00 7.00E+00 8.00E+00 9.00E+00 1.00E+01 1.20E+01 1.50E+01 2.00E+01
3.00E+01 4.00E+01 5.00E+01 7.50E+01 1.00E+02 1.50E+02 2.00E+02
1.50E-19 3.50E-19 8.00E-19 1.50E-18 2.70E-18 3.80E-18 5.20E-18 6.20E-18
7.80E-18 9.20E-18 8.00E-18 7.00E-18 6.20E-18 5.50E-18 4.40E-18 3.50E-18
2.20E-18 1.50E-18 8.70E-19 2.60E-19 1.10E-19 3.20E-20 1.40E-20
20 1.80 02 B1SIG
1.80E+00 1.90E+00 2.00E+00 2.30E+00 2.60E+00 3.00E+00 3.50E+00 4.50E+00
6.00E+00 8.00E+00 1.00E+01 1.50E+01 2.00E+01 3.00E+01 5.00E+01 6.00E+01
8.00E+01 1.00E+02 1.50E+02 2.00E+02
6.30E-20 1.30E-19 2.00E-19 4.60E-19 7.10E-19 1.00E-18 1.35E-18 1.80E-18
1.97E-18 1.90E-18 1.65E-18 1.25E-18 1.00E-18 6.40E-19 2.40E-19 1.40E-19
5.90E-20 3.00E-20 8.90E-21 3.80E-21
29 4.70 02 A3SIG
4.70E+00 4.80E+00 5.00E+00 5.50E+00 6.00E+00 7.00E+00 8.00E+00 1.00E+01
1.20E+01 1.50E+01 2.00E+01 2.50E+01 3.00E+01 4.00E+01 5.00E+01 7.50E+01
1.00E+02 1.50E+02 2.00E+02 3.00E+02 5.00E+02 7.50E+02 1.00E+03 1.50E+03
2.00E+03 3.00E+03 5.00E+03 7.00E+03 1.00E+04
1.00E-18 5.40E-18 8.20E-18 1.25E-17 1.50E-17 1.65E-17 1.64E-17 1.50E-17
1.30E-17 1.10E-17 8.50E-18 7.00E-18 6.00E-18 4.80E-18 3.80E-18 2.60E-18
2.05E-18 1.40E-18 1.10E-18 7.60E-19 4.90E-19 3.30E-19 2.60E-19 1.75E-19
1.30E-19 8.80E-20 5.30E-20 3.80E-20 2.60E-20
30 8.50 02 B3SIG
8.50E+00 8.75E+00 9.00E+00 9.50E+00 1.00E+01 1.10E+01 1.30E+01 1.50E+01
1.80E+01 2.20E+01 2.50E+01 3.00E+01 4.00E+01 5.00E+01 7.50E+01 1.00E+02
1.50E+02 2.00E+02 3.00E+02 5.00E+02 7.50E+02 1.00E+03 1.50E+03 2.00E+03
3.00E+03 5.00E+03 7.50E+03 1.20E+04 2.00E+04 3.00E+04
2.80E-19 1.00E-18 2.30E-18 6.60E-18 1.25E-17 2.50E-17 5.00E-17 7.00E-17
8.90E-17 1.02E-16 1.07E-16 1.10E-16 1.06E-16 1.00E-16 8.30E-17 7.20E-17
5.30E-17 4.60E-17 3.40E-17 2.45E-17 1.86E-17 1.50E-17 1.10E-17 9.00E-18
6.60E-18 4.40E-18 3.10E-18 2.00E-18 1.30E-18 8.80E-19
```

Table A5 (Cont'd) - Cross sections

```
29 11.0 02 '9.9'
1.10E+01 1.15E+01 1.20E+01 1.30E+01 1.50E+01 1.70E+01 2.00E+01 2.30E+01
3.00E+01 4.00E+01 5.00E+01 6.00E+01 8.00E+01 1.00E+02 1.50E+02 2.00E+02
3.00E+02 5.00E+02 7.50E+02 1.00E+03 1.50E+03 2.00E+03 3.00E+03 5.00E+03
7.00E+03 1.00E+04 1.50E+04 2.50E+04 5.00E+04
2.00E-20 5.50E-20 1.10E-19 2.70E-19 6.00E-19 1.20E-18 1.85E-18 2.70E-18
3.20E-18 3.70E-18 3.80E-18 3.75E-18 3.45E-18 3.15E-18 2.60E-18 2.20E-18
1.70E-18 1.20E-18 9.10E-19 7.50E-19 5.50E-19 4.45E-19 3.20E-19 2.20E-19
1.60E-19 1.20E-19 8.40E-20 5.40E-20 2.80E-20
27 14.0 02 RYD1
1.40E+01 1.50E+01 1.60E+01 1.70E+01 1.80E+01 2.00E+01 2.50E+01 3.00E+01
4.00E+01 5.00E+01 7.00E+01 1.00E+02 1.50E+02 2.00E+02 3.00E+02 5.00E+02
7.50E+02 1.00E+03 1.50E+03 2.00E+03 3.00E+03 5.00E+03 7.50E+03 1.00E+04
1.50E+04 2.50E+04 5.00E+04
9.00E-19 1.60E-18 3.30E-18 7.00E-18 1.25E-17 2.50E-17 6.20E-17 9.00E-17
1.27E-16 1.45E-16 1.50E-16 1.40E-16 1.25E-16 1.05E-16 8.50E-17 6.00E-17
4.50E-17 3.70E-17 2.80E-17 2.30E-17 1.65E-17 1.10E-17 8.00E-18 6.30E-18
4.50E-18 3.00E-18 1.70E-18
30 18.7 02 RYD2
2.20E+01 2.50E+01 3.00E+01 4.00E+01 5.00E+01 6.00E+01 7.00E+01 8.00E+01
9.00E+01 1.00E+02 1.50E+02 2.00E+02 3.00E+02 4.00E+02 5.00E+02 6.00E+02
7.00E+02 8.00E+02 9.00E+02 1.00E+03 1.20E+03 1.60E+03 2.00E+03 3.00E+03
5.00E+03 7.00E+03 1.00E+04 2.00E+04 3.00E+04 5.00E+04
1.30E-18 3.50E-18 1.00E-17 2.81E-17 4.49E-17 5.97E-17 6.95E-17 7.97E-17
8.61E-17 9.21E-17 1.00E-16 9.56E-17 8.13E-17 6.77E-17 5.64E-17 4.93E-17
4.40E-17 3.97E-17 3.64E-17 3.37E-17 2.90E-17 2.40E-17 2.00E-17 1.40E-17
9.60E-18 7.20E-18 5.40E-18 3.10E-18 2.20E-18 1.50E-18
22 17.6 02 989
1.70E+01 1.80E+01 2.00E+01 2.50E+01 3.00E+01 4.00E+01 5.00E+01 6.00E+01
7.00E+01 8.00E+01 9.00E+01 1.00E+02 1.20E+02 1.40E+02 1.60E+02 1.80E+02
2.00E+02 2.20E+02 2.40E+02 2.60E+02 2.80E+02 3.00E+02
2.53E-20 6.00E-20 1.39E-19 3.20E-19 4.81E-19 8.74E-19 1.27E-18 1.62E-18
1.82E-18 1.93E-18 1.94E-18 1.93E-18 1.87E-18 1.80E-18 1.71E-18 1.62E-18
1.53E-18 1.46E-18 1.39E-18 1.33E-18 1.27E-18 1.21E-18
25 17.2 021027
1.50E+01 1.60E+01 1.70E+01 1.80E+01 1.90E+01 2.00E+01 2.50E+01 3.00E+01
4.00E+01 5.00E+01 6.00E+01 7.00E+01 8.00E+01 9.00E+01 1.00E+02 1.20E+02
1.40E+02 1.60E+02 1.80E+02 2.00E+02 2.20E+02 2.40E+02 2.60E+02 2.80E+02
3.00E+02
1.00E-21 5.00E-21 2.50E-20 7.00E-20 1.00E-19 1.30E-19 2.60E-19 3.80E-19
6.20E-19 8.90E-19 1.12E-18 1.32E-18 1.44E-18 1.47E-18 1.47E-18 1.44E-18
1.39E-18 1.33E-18 1.27E-18 1.21E-18 1.15E-18 1.09E-18 1.05E-18 9.95E-19
9.50E-19
20 14.6 021304
1.47E+01 2.00E+01 3.00E+01 4.00E+01 5.00E+01 6.00E+01 7.00E+01 8.00E+01
9.00E+01 1.00E+02 1.20E+02 1.40E+02 1.60E+02 1.80E+02 2.00E+02 2.20E+02
2.40E+02 2.60E+02 2.80E+02 3.00E+02
7.00E-19 1.40E-18 2.28E-18 2.63E-18 3.25E-18 3.50E-18 3.75E-18 3.90E-18
3.80E-18 3.70E-18 3.50E-18 3.25E-18 3.08E-18 2.89E-18 2.72E-18 2.58E-18
2.45E-18 2.31E-18 2.20E-18 2.10E-18
20 14.2 021356
1.40E+01 2.00E+01 3.00E+01 4.00E+01 5.00E+01 6.00E+01 7.00E+01 8.00E+01
9.00E+01 1.00E+02 1.20E+02 1.40E+02 1.60E+02 1.80E+02 2.00E+02 2.20E+02
2.40E+02 2.60E+02 2.80E+02 3.00E+02
6.00E-19 1.30E-18 2.40E-18 3.40E-18 4.65E-18 5.50E-18 6.25E-18 6.60E-18
6.80E-18 7.00E-18 6.90E-18 6.70E-18 6.45E-18 6.20E-18 5.95E-18 5.70E-18
5.45E-18 5.20E-18 5.05E-18 4.95E-18
```

Table A5 (Cont'd) - Cross sections

```
OI

  1.40E+01 8.00E+00 OI ION
1.40E+01 1.50E+01 1.60E+01 1.80E+01 2.00E+01 2.50E+01 3.00E+01 4.00E+01
6.00E+01 7.00E+01 1.00E+02 1.50E+02 2.50E+02 4.00E+02 6.00E+02 8.00E+02
1.00E+03 1.50E+03 2.00E+03 3.00E+03 5.00E+03 7.50E+03 1.00E+04 1.50E+04
2.50E+04 5.00E+04
1.50E-18 6.50E-18 1.55E-17 3.70E-17 5.60E-17 8.60E-17 1.05E-16 1.30E-16
1.45E-16 1.53E-16 1.50E-16 1.40E-16 1.15E-16 9.00E-17 7.00E-17 6.10E-17
5.50E-17 4.30E-17 3.80E-17 3.00E-17 2.30E-17 1.90E-17 1.60E-17 1.09E-17
1.00E-18 4.20E-18
20 2.10 OI 1D
2.10E+00 2.20E+00 2.40E+00 2.60E+00 2.90E+00 3.50E+00 4.00E+00 5.00E+00
6.00E+00 7.00E+00 8.50E+00 1.00E+01 1.50E+01 2.50E+01 4.00E+01 6.00E+01
9.00E+01 1.00E+02 1.50E+02 2.00E+02 3.00E+02
1.00E-18 2.50E-18 6.00E-18 1.00E-17 1.50E-17 2.25E-17 2.53E-17 2.75E-17
2.75E-17 2.69E-17 2.48E-17 2.33E-17 1.80E-17 1.30E-17 8.20E-18 5.00E-18
3.30E-18 2.00E-18 1.00E-18 5.00E-19 1.50E-19
18 4.00 OI 1S
4.00E+00 4.50E+00 5.00E+00 6.00E+00 7.00E+00 8.00E+00 9.00E+00 1.00E+01
1.20E+01 1.50E+01 2.00E+01 3.00E+01 4.00E+01 5.00E+01 7.00E+01 1.00E+02
1.50E+02 2.00E+02 3.00E+02 5.00E+02
1.00E-19 3.00E-19 9.50E-19 1.50E-18 1.90E-18 2.20E-18 2.35E-18 2.40E-18
2.40E-18 2.20E-18 1.90E-18 1.40E-18 1.10E-18 9.00E-19 6.50E-19 4.00E-19
2.00E-19 1.20E-19 5.00E-20
16  9.1 OI 5S
9.80E+00 1.00E+01 1.10E+01 1.20E+01 1.30E+01 1.40E+01 1.50E+01 1.60E+01
1.80E+01 2.20E+01 2.50E+01 3.00E+01 4.00E+01 5.00E+01 7.00E+01 1.00E+02
1.10E-18 2.50E-18 6.00E-18 1.20E-17 1.85E-17 2.35E-17 2.50E-17 2.45E-17
2.35E-17 1.78E-17 1.38E-17 9.00E-18 4.40E-18 2.20E-18 7.50E-19 2.75E-19
24 10.1 OI 3S
1.00E+01 1.20E+01 1.40E+01 1.70E+01 2.20E+01 3.00E+01 5.00E+01 7.50E+01
1.00E+02 1.50E+02 2.00E+02 3.00E+02 5.00E+02 7.50E+02 1.00E+03 1.50E+03
2.00E+03 3.00E+03 5.00E+03 7.00E+03 1.00E+04 1.50E+04 2.50E+04 5.00E+04
6.00E-18 2.30E-17 4.70E-17 5.30E-17 5.40E-17 4.90E-17 4.00E-17 3.30E-17
2.90E-17 2.30E-17 2.00E-17 1.50E-17 1.05E-17 8.00E-18 6.20E-18 4.80E-18
3.80E-18 2.80E-18 1.80E-18 1.40E-18 1.00E-18 7.20E-19 4.60E-19 2.60E-19
27 15.0 OI 3DRYD
1.50E+01 1.55E+01 1.60E+01 1.70E+01 1.80E+01 2.00E+01 2.50E+01 3.00E+01
4.00E+01 5.00E+01 7.00E+01 1.00E+02 1.50E+02 2.00E+02 3.00E+02 5.00E+02
7.50E+02 1.00E+03 1.50E+03 2.00E+03 3.00E+03 5.00E+03 7.50E+03 1.00E+04
1.50E+04 2.50E+04 5.00E+04
1.00E-20 6.00E-20 1.50E-19 4.50E-19 1.00E-18 2.30E-18 6.40E-18 1.00E-17
1.50E-17 1.70E-17 1.80E-17 1.75E-17 1.50E-17 1.30E-17 1.03E-17 7.40E-18
5.60E-18 4.50E-18 3.50E-18 2.80E-18 2.10E-18 1.50E-18 1.13E-18 9.00E-19
6.60E-19 4.60E-19 2.85E-19
21 14.5 OI 1DRYD
1.45E+01 1.50E+01 1.60E+01 1.70E+01 1.80E+01 1.90E+01 2.00E+01 2.20E+01
2.50E+01 3.00E+01 3.50E+01 4.00E+01 5.00E+01 7.00E+01 1.00E+02 1.50E+02
2.00E+02 3.00E+02 5.00E+02 7.50E+02 1.00E+03
1.00E-18 7.00E-18 1.70E-17 2.10E-17 2.60E-17 2.80E-17 3.00E-17 3.10E-17
2.90E-17 2.60E-17 2.20E-17 1.80E-17 1.30E-17 7.00E-18 4.00E-18 1.80E-18
1.00E-18 4.80E-19 1.80E-19 7.50E-20 4.30E-20
12 00.0 OII 4P
2.54E+01 2.85E+01 3.19E+01 3.58E+01 4.51E+01 5.68E+01 7.15E+01 9.00E+01
1.13E+02 1.43E+02 1.80E+02 2.84E+02
1.15E-18 4.54E-18 7.98E-18 1.16E-17 1.89E-17 2.58E-17 3.15E-17 3.45E-17
3.58E-17 3.48E-17 3.29E-17 2.66E-17
11 00.0 OII 2P
3.70E+01 4.00E+01 4.48E+01 5.03E+01 6.33E+01 7.97E+01 1.00E+02 1.26E+02
1.59E+02 2.00E+02 2.52E+02
1.02E-19 3.38E-19 7.77E-19 1.32E-18 2.61E-18 4.02E-18 5.21E-18 5.85E-18
6.05E-18 5.99E-18 5.58E-18
```

Table A5 (Cont'd) - Cross sections

```
N
05
28 10.9 N 1134
1.13E+01 1.20E+01 1.30E+01 1.40E+01 1.50E+01 1.70E+01 2.00E+01 2.10E+01
2.20E+01 2.50E+01 3.00E+01 4.00E+01 5.00E+01 6.00E+01 7.00E+01 8.00E+01
9.00E+01 1.00E+02 1.20E+02 1.40E+02 1.60E+02 1.80E+02 2.00E+02 2.20E+02
2.40E+02 2.60E+02 2.80E+02 3.00E+02
1.20E-17 1.30E-16 1.60E-16 1.70E-16 1.76E-16 1.84E-16 1.92E-16 1.92E-16
1.90E-16 1.82E-16 1.68E-16 1.37E-16 1.14E-16 1.00E-16 8.80E-17 8.00E-17
7.20E-17 6.80E-17 6.00E-17 5.40E-17 4.94E-17 4.54E-17 4.20E-17 3.90E-17
3.64E-17 3.40E-17 3.20E-17 3.00E-17
26 10.3 N 1200
1.13E+01 1.20E+01 1.30E+01 1.40E+01 1.50E+01 1.70E+01 2.00E+01 2.50E+01
3.00E+01 4.00E+01 5.00E+01 6.00E+01 7.00E+01 8.00E+01 9.00E+01 1.00E+02
1.20E+02 1.40E+02 1.60E+02 1.80E+02 2.00E+02 2.20E+02 2.40E+02 2.60E+02
2.80E+02 3.00E+02
1.25E-17 7.50E-17 1.15E-16 1.38E-16 1.55E-16 1.88E-16 2.15E-16 2.50E-16
2.55E-16 2.45E-16 2.25E-16 2.03E-16 1.93E-16 1.83E-16 1.70E-16 1.63E-16
1.44E-16 1.31E-16 1.21E-16 1.13E-16 1.05E-16 9.80E-17 9.18E-17 8.63E-17
8.15E-17 7.75E-17
17 10.0 N 1243
1.30E+01 1.40E+01 1.50E+01 1.60E+01 1.70E+01 1.80E+01 1.90E+01 2.00E+01
2.50E+01 3.00E+01 4.00E+01 5.00E+01 6.00E+01 7.00E+01 8.00E+01 9.00E+01
1.00E+02
5.50E-19 2.48E-18 4.57E-18 5.06E-18 5.39E-18 5.40E-18 5.50E-18 5.34E-18
4.13E-18 3.58E-18 2.97E-18 2.69E-18 2.42E-18 2.23E-18 2.08E-18 1.90E-18
1.76E-18
18  8.3 N 1493
1.20E+01 1.30E+01 1.40E+01 1.50E+01 1.60E+01 1.70E+01 1.80E+01 1.90E+01
2.00E+01 2.50E+01 3.00E+01 4.00E+01 5.00E+01 6.00E+01 7.00E+01 8.00E+01
9.00E+01 1.00E+02
1.09E-18 4.35E-18 1.16E-17 2.29E-17 3.46E-17 3.63E-17 3.63E-17 3.35E-17
3.15E-17 2.18E-17 1.85E-17 1.40E-17 1.27E-17 1.18E-17 1.11E-17 1.05E-17
1.01E-17 9.60E-18
18  7.1 N 1744
1.20E+01 1.30E+01 1.40E+01 1.50E+01 1.60E+01 1.70E+01 1.80E+01 1.90E+01
2.00E+01 2.50E+01 3.00E+01 4.00E+01 5.00E+01 6.00E+01 7.00E+01 8.00E+01
9.00E+01 1.00E+02
3.90E-19 1.56E-18 4.16E-18 8.19E-18 1.24E-17 1.30E-17 1.30E-17 1.20E-17
1.13E-17 7.80E-18 6.63E-18 5.00E-18 4.45E-18 4.23E-18 3.97E-18 3.77E-18
3.62E-18 3.44E-18
```

REFERENCES

Anderson, D. E., Jr., P. D. Feldman, E. P. Gentieu and R. R. Meier, The UV dayglow 3, OI emission at 989, 1027, 1152, 1304, and 1356 Å, Geophys. Res. Lett., 7, 1057, 1980.

Borst, W. L., Excitation of several important metastable states of N_2 by electron impact, Phys. Rev., 5, 648, 1972.

Cartwright, D. C., S. Trajmar, A. Chutjian and W. Williams, Electron impact excitation of the electronic states of N_2. II. Integral cross sections at incident energies from 10 to 50 eV, Phys. Res., 1041, 1977.

Davis, J. and M. Blaha, Electron collision excitation of metastable levels in NI, NII, OI, OII, OIII, submitted to Phys. Rev., 1976.

Donnelly, R. F. and J. H. Pope, The 1-3000Å solar flux for a moderate level of solar activity for use in modeling the ionosphere and upper atmosphere, NOAA Tech. Rept., ERL 276, 1973.

Feldman, P. D., D. E. Anderson, R. R. Meier and E. P. Gentieu, The ultraviolet dayglow 4. The spectrum and excitation of singly ionized oxygen, J. Geophys. Res., 86, 3538, 1981.

Fite, W. L. and R. T. Brackmann, Ionization of atomic oxygen on electron impact, Phys. Rev., 113, 815, 1959.

Gentieu, E. P., P. D. Feldman and R. R. Meier, Spectroscopy of the extreme ultraviolet dayglow at 6.5 Å resolution: Atomic and ionic emissions between 530 and 1240 Å, Geophys. Res. Lett., 6, 325, 1979.

Gentieu, E. P., P. D. Feldman, R. W. Eastes and A. B. Christensen, Spectroscopy of the extreme ultraviolet dayglow during active solar conditions, Geophys. Res. Lett., 8, 12, 1981.

Green, A. E. S. and R. S. Stolarski, Analytic models of electron impact excitation cross sections, J. Atmos. Terr. Phys., 34, 1703, 1972.

Hake, R. D. Jr., and A. V. Phelps, Momentum transfer and inelastic collision cross sections for electrons in O_2, CO and CO_2, Phys. Rev., 158, 70, 1967.

Henry, R. J., P. G. Burke, and A. L. Sinfailam, Scattering of electrons by C, N, O, N+, O+, and O^{2+}, Phys. Rev., 178, 218, 1969.

Huffman, R. E., F. J. LeBlanc, J. C. Larrabee and D. E. Paulsen, Satellite vacuum ultraviolet airglow and auroral observations, J. Geophys. Res., 85, 2201, 1980.

Jacchia, L. G., Revised static models of the thermosphere and exosphere with empirical temperature profiles, Smithsonian Astrophys. Obs. Spec. Rept., 332, 1971.

Jacchia, L. G., Thermospheric temperature, density and composition: New models, Smithsonian Astrophys. Obs. Spec. Rept., 375, 1977.

Kieffer, L. J. and G. H. Dunn, Electron impact ionization cross-section data for atmos. atomic ions, and diatomic molecules - I. Experimental data, Rev. Mod. Phys., 38, 1966.

Kirby, K., E. R. Constantinides, S. Babeu, M. Oppenheimer and G. A. Victor, Photoionization and photoabsorption cross sections of He, O, N_2, and O_2 for aeronomic calculations, At. Data Nucl. Tables, 23, 63, 1979.

Lee, J. S., J. P. Doering, T. A. Potemra and L. H. Brace, Measurements of the ambient photoelectron spectrum from Atmospheric Explorer: 1. AE-E measurements below 300 km during solar minimum conditions, Planet. Space Sci., 28, 947, 1980.

McLaughlin, R. W., Vacuum ultra-violet and visible radiation from electron impact excitation of nitrogen, hydrogen, oxygen, the light hydrocarbons and the rare gases, Thesis, University of Pittsburgh, Pittsburgh, PA, U.S.A., 1977.

Meier, R. R., D. J. Strickland, P. D. Feldman and E. P. Gentieu, The ultraviolet dayglow 1, far UV emissions of N and N_2, J. Geophys. Res., 85, 2177, 1980.

Mumma, M. J. and E. C. Zipf, Dissociative excitation of vacuum ultraviolet emission features by electron impact on molecular gases I H_2 and O_2, J. Chem. Phys., 1661, 55, 1971a.

Mumma, M. J. and E. C. Zipf, Dissociative excitation of vacuum ultraviolet emissions featured by electron impact on molecular gases, II N_2, J. Chem. Phys., 558, 12, 1971b.

Oran, E. S. and D. J. Strickland, Photoelectron flux in the Earth's ionosphere, Planet. Space Sci., 26, 1161, 1978.

Peach, G., Ionization of neutral atoms with outer 2p, 3s and 3p eletrons by electron and proton impact, J. Phys., 328, 3, 1970.

Rapp, D. and P. Englander-Golden, Total cross sections for ionization and attachment in gases by electron impact - II. Negative ion formation, J. Chem. Phys., 43, 1480, 1965.

Rapp, D., P. Englander-Golden and D. D. Brigilia, Cross sections for dissociative ionization of molecules by electron impact, J. Chem. Res., 42, 4081, 1965.

Schulz, G. J., Vibrational excitation of N_2, CO and H_2 by electron impact, Phys. Rev., 135, 988, 1964.

Schulz, G. J. and J. T. Dowell, Excitation of vibrational electron levels in O_2 by electron impact, Phys. Rev., 128, 174, 1962

Shunk, R. W. and P. B. Hayes, Photoelectron energy losses to thermal electrons, Planet. Space Sci., 19, 113, 1971.

Silverman, S. M. and E. N. Lassettre, Electronic collision cross sections, for oxygen at excitation energies above 10 volts, Report No. 7, Ohio State Dept. of Chem. Sci., 1957.

Stone, E. J. and E. C. Zipf, Excitation of atomic nitrogen by electron impact, J. Chem. Phys., 58, 4278, 1973.

Stone, E. J. and E. C. Zipf, Electron-impact excitation of the $^3S^\circ$ and $^5S^\circ$ states of atomic oxygen, J. Chem. Phys., 60, 11, 1974.

Strickland, D. J., D. L, Book, T. P. Coffey and J. A. Fedder, Transport equation techniques for the deposition of auroral electrons, J. Geophys. Res., 81, 2755, 1976.

Torr, M. R., D. G. Torr, R. A. Ong and H. E. Hinteregger, Ionization frequencies for major thermospheric constituents as a function of solar cycle 21, Geophys. Res. Lett., 6, 771, 1979.

Trajmar, S., D. C. Cartwright and W. Williams, Differential and integral cross sections for electron impact excitation of the $a\,^1\Delta_g$ and $b\,^1\Sigma_g^+$ states of O_2, Phys. Rev., 4, 1482, 1971.

Trajmar, S., W. Williams and A. Kupperman, Angular dependence of electron impact excitation cross sections of O_2, J. Chem Phys., 56, 3759.

Watson, C. E., V. A. Dulock, Jr., R. S. Stolarski and A. E. S. Green, Electron impact cross sections for atmospheric species III. molecular oxygen, J. Geophys. Res., 72, 3961, 1967.

Wong, S. F., M. J. Boness, and G. J. Schulz, Vibrational excitation of O_2 by electron impact above 4eV, Phys. Rev. Lett., 31, 969, 1973.

Zipf, E. C. and M. R. Gorman, Electron impact excitation of the singlet states of N_2. I. The Birge-Hopfield system, ($b\,^1\Pi_u$-$X\,^1\Sigma_g^+$), J. Chem. Phys., 73, 813, 1980.

Zipf, E. C., R. W. McLaughlin and M. R. Gorman, A study of the excitation and radiative decay of the $3s'\,^3D^\circ$ and $3d\,^3D^\circ$ levels of atomic oxygen, Planet. Space Sci., 27, 719, 1979.